

Comparison of Horizontal Ground Source (Geothermal) Heat Pump Layouts for Optimal Performance and Thermal Efficiency

By

Elizabeth Bocchino

* * * * *

Submitted in partial fulfillment

Of the requirements for

Honors in the Department of Mechanical Engineering

UNION COLLEGE

June 2011

ABSTRACT

BOCCHINO, ELIZABETH Comparison of Horizontal Ground Source (Geothermal) Heat Pump Layouts for Optimal Performance and Thermal Efficiency. Department of Mechanical Engineering, June 2011

ADVISOR: Professor Ann Anderson, PhD

This study investigates the difference in thermal efficiencies of horizontal ground source heat pump layouts through computer simulation and experimental modeling. The main objective of this project was to determine if the shape of the layout affects the total heat exchange in a horizontal geothermal system. Geothermal energy is power extracted from the Earth and studies have been focused on increasing the efficiency of the heat transfer from the Earth to the system. Steady state and transient thermal analyses were conducted on two horizontal layout shapes, a U-loop and a coil, in ANSYS Fluent. This system was not full size, both of the layouts were about 2.1 meters in length. The steady state analyses show that the coil shape is more efficient with a steady state heat transfer rate of 8.3 W, compared to 7.5 W produced by the U-loop. A transient simulation was also conducted for each layout and the results were dependent upon initial conditions. Setting different initial conditions to the soil and the working fluid resulted in slightly higher heat transfer rates initially. An experimental model of the coil layout was constructed and the results were compared to the results of the ANSYS simulations. The results from the experimental testing were inconclusive. However, for the conditions tested in the computational analyses, the coil shape produced more heat transfer than the U-loop shape, indicating that the shape of the layout does affect the total heat transfer, due to carry over heating through the soil.

Table of Contents

Chapter 1: Introduction	1
Geothermal Background	1
Literature Review	6
Chapter 2: Computational Fluid Dynamic Verification Studies	12
Shape Factor Verification	13
Energy Balance Verification	16
Chapter 3: Layout Studies	19
Material Properties	19
Layouts	21
U-Loop Simulation	22
Steady State Results	26
Transient Results	27
Coil Simulation	29
Steady State Results	30
Transient Results	31
Slinky Simulation	33
Chapter 4: Experimental Model	37
Test Apparatus	37
Experimental Procedure	42
Experimental Results	43
Experimental Computational Fluid Dynamic Results	44
Experimental Test Results	45
Water Test	46
Antifreeze Test	47
Experimental Conclusions	48
Chapter 5: Conclusions and Future Work	50
Conclusions	50
Future Work	50
Appendix A: Challenges	
Appendix B: ANSYS Simulation Report	

Figures

Figure 1 - Ground Source Heat Pump in Heating Mode	3
Figure 2 - Types of Geothermal Loops.....	4
Figure 3 – Mesh of Simulation Model of a U-loop Pair	9
Figure 4 – Test Cube Model with Simulation Mesh.....	13
Figure 5 - Types of Geothermal Loops.....	14
Figure 6 – Shape Factor vs. Simulation for Diameter 0.01m	15
Figure 7 – Shape Factor vs. Simulation for Diameter 0.02m	16
Figure 8 – U – Loop Energy Balance and Boundary Conditions	17
Figure 9 – U – Loop Layout	21
Figure 10 – Coil Layout.....	21
Figure 11 – Slinky Layout	21
Figure 12 – U – Loop Layout Dimensions	22
Figure 13 – U – Loop Soil Plot Dimensions.....	23
Figure 14 –U – Loop Steady State Simulation Results.....	26
Figure 15 – U – Loop Heat Transfer First Method Transient Simulation Results	28
Figure 16 – U – Loop Heat Transfer Second Method Transient Simulation Results	28
Figure 17 – Coil Layout Dimensions.....	29
Figure 18 – Coil Soil Plot Dimensions	30
Figure 19 – Temperature Distribution for Coil Steady State Simulation	31
Figure 20 – Coil Heat Transfer First Method Transient Simulation Results.....	32
Figure 21 – Coil Heat Transfer Second Method Transient Simulation Results	33
Figure 22 – Slinky Coil Layout	34
Figure 23 – Tempertaure Distribution Comparison Between U-Loop and Coil	35
Figure 24 – Solidworks Drawing of Experimental Test Apparatus.....	37
Figure 25 – Finished Experimental Test Apparatus	38
Figure 26 – Top View of Thermocouple Placement.....	40
Figure 27 – Side View of Thermocouple Placement.....	40
Figure 28 – Schematic of Experimental Test Apparatus Setup	41

Figure 29 – Test Apparatus Unit.....	41
Figure 30 – Data Acquisition System and Digital Reader	41
Figure 31 – Test System	42
Figure 32 – Pump and Heating Systems	42
Figure 33 – Experimental Simulation Predicting Heat Transfer of Experimental Setup	45
Figure 34 – Soil Temperatures from Water Test	46
Figure 35 – Soil Temperatures from Antifreeze Test	47

Tables

Table 1 – Literature Research	7
Table 2 – Shape Factor Boundary Condition Values	14
Table 3 – Shape Factor vs. Simulation Results for Diameter 0.01m	14
Table 4 – Shape Factor vs. Simulation Results for Diameter 0.02m	15
Table 5 – Simulation Properties and Results	17
Table 6 – Material Properties	20
Table 7 – Thermal Conductivities of Soil	21
Table 8 – Reynold’s Number Classifications	24
Table 9 – Simulation Properties	24
Table 10 – Flow Classification	24
Table 11 – U-loop Simulation Properties	27
Table 12 – Coil Simulation Properties	31

Chapter 1: Introduction

Does the shape of a horizontal ground source heat pump (GSHP) layout affect the total heat transfer from the soil to the working fluid, if so what is the optimal layout? This study investigates the difference in thermal efficiencies of horizontal ground source heat pump layouts through computer simulation and experimental modeling. A GSHP is comprised of several main parts, the layout, or system of buried tubes, the ground that the layout is installed in, the working fluid that runs through the layout and the heat exchanger that extracts the energy from the working fluid. The main objective of this project is to determine if the shape of the layout affects the total heat exchange in a horizontal geothermal system.

There is a lack of scientific data in the literature proving one layout to be more efficient than another and current industry practice is to use “rules of thumb” to decide which layout to install for customers. These rules of thumb are based almost entirely on environmental conditions and are presumed to be reliable despite the lack of supporting data. It is hypothesized that the layout with the most bends per square foot will be the most thermally efficient due to a more turbulent flow within the tubing.

Background on Geothermal Systems

Geothermal energy is power extracted from the Earth. Although not a new technology, recent efforts have been made in improving the efficiencies of geothermal systems. Studies have been focused on increasing the efficiency of heat transfer from the Earth to the system. Efficiencies are rising due to

new technologies such as; thermally advanced materials, grout, and increased borehole conductivity. Extended research in this area is making residential geothermal systems an affordable investment for a family and a remarkable alternative energy source.

Geothermal energy has a long history. The first people in North America to take advantage of geothermal resources were the Paleo-Indians, 10,000 years ago. (Geothermal Technologies, 2006) They discovered natural hot springs which were used for bathing and the waters were even believed to have healing properties. It was 1921, when John Grant generated electric energy from the drilling of wells. His plan successfully generated 250 kilowatts of electricity, but the geothermal power plant was not competitive with other sources of energy and was closed. However, in 1930 the first commercial greenhouse use of geothermal energy was established in Boise, Idaho. (Geothermal Technologies, 2006) Engineers have been working since then to increase the efficiency of this old technology and harness its energy for smaller, single well projects such as residential homes.

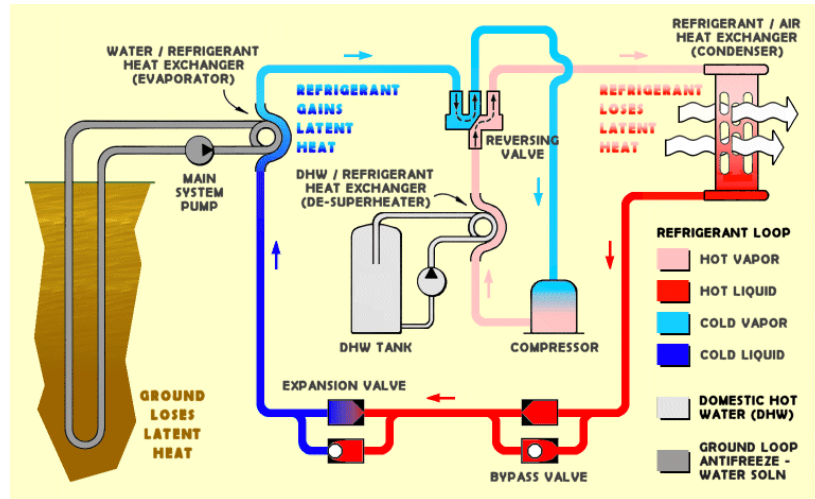


Figure 1 - Ground Source Geothermal Heat Pump in Heating Mode showing the working fluid gaining heat from the ground and the heat exchanger removing the collected heat <http://www.geo4va.vt.edu/A3/A3.htm>

A typical geothermal system includes the following components (see figure 1): the heat pump unit, including the compressor and heat exchanger; a heat exchanging medium (fluid running through the system); and the air delivery system. When operating, the heat exchanger medium flows through the loops (piping) underground and removes some of the Earth's natural heat. It is then pumped through the compressor and the heat exchanger, where the heat is extracted from the fluid. This heat is then distributed through the home via an air delivery system. (Natural, 2009)

There are two types of geothermal systems, open loop and closed loop. Open loop systems use surface water or a well as the heat exchange fluid and circulate that fluid back to the original source. Closed loop systems have a fluid that is continuously circulated through the system.

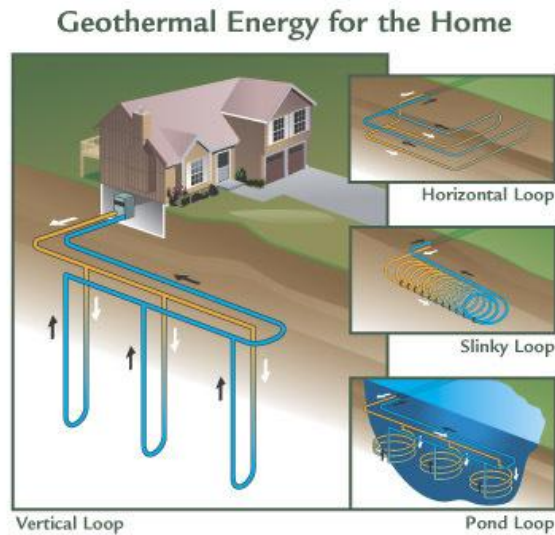


Figure 2 – Types of Geothermal Loops
http://www.thermalairllc.com/geothermal_heat_pumppic.jpg

There are several types of closed loop systems with varying loop design: horizontal, vertical, and, pond (see figure 2). The horizontal layouts involve less digging and can be more cost effective, but a large plot of land is needed. The trenches are no more than 4-6 feet deep and two loops are usually set side by side at different depths for the most effective heat transfer. The vertical layout involves digging to a greater depth, but the land requirement or footprint is much less. Vertical systems are applicable in many renovation projects where land is limited. The pond or lake option involves no digging, utilizing the depth of a body of water on site as the heat source. The loops are submerged in the body of water, but more often than not there is still a secondary heat exchanger fluid circulating through the piping, making it a closed loop system. Pond systems often can be the most

cost effective option for clients because it involves no drilling or digging.

(Geothermal)

There are a few myths about the geothermal energy industry in general. It is believed that geothermal energy is extremely expensive and the return on investment is very large. That was true 15 years ago, but now the most expensive part of the process is drilling or digging, and with new technology shallower wells are being drilled, which have the same performance rates as systems with deeper wells. This reduces the cost, making the return on investment about 3 years and systems much more affordable.

A second myth is about the location of geothermal wells. Geothermal energy is applicable everywhere and ambient temperatures are found about 1-2 feet below the frost line in most locations. Both horizontal and vertical systems require about 150-220 feet of piping to support a 1.5 ton (approximately 3000W) system. The difference is that vertical systems require that length in depth and horizontal systems require that length in a trench only 4-5 feet in depth. Also geothermal does not have to be installed in only new construction projects, many geothermal installations are retro-fittings for older homes looking to upgrade their heating and cooling systems. These systems can be very cost effective and suitable for a residential home and the advances in technology are only improving on the overall cost and efficiency of the systems. (Debunking, 2010)

Literature Review

Much research has been done on GSHPs, both horizontal and vertical; however, it typically focuses on system efficiencies or borehole design. Many of these studies utilized computational modeling supplemented by experimental research (see table 1). Studies have been conducted in both Turkey and Japan on geothermal systems using computational modeling and ideas from those studies inspired the use of computation models in this research. Esen et al. (2007) performed numerical modeling to determine the temperature distribution in the vicinity of the pipe of a horizontal geothermal system. A second study by Nam et al. (2008) used computational modeling to predict heat transfer rates of a vertical GSHP; their tests were successful with very low error. A third study by Hepbasli et al. (2001) was conducted on a vertical closed U-loop system to test the performance characteristics of a system and their efficiency. The positive results of these studies lead to establishing similar testing techniques for this study.

Table 1 – Literature Research

Comparison of Geothermal Horizontal Closed Loop Systems								
Article Source	Location	Hypothesis Tested	System Tested (Horiz/Vert, Open/Closed, Shapes)	Working Fluid	Test Method (Lab verses full scale)	Simulation type	Full Scale Pump System or Only One Part	Results
[1]	Tianjin, PR China	Ground thermal conductivity and evaluation of the thermal performance of borehole heat exchangers of GSHP	Vertical Borehole, Closed U-loop	R22 Refrigerant	In situ thermal tests which was the base temperature distribution for the lab tests	No computer simulations	Full Scale	Thermal testing is crucial in determining the conductivity of the ground
[2]	Ege University, Izmir, Turkey	Test the performance characteristics of the GSHP	Vertical, Closed U-loop	R22 Refrigerant	In situ tests, 65 sq meter room	no computer simulations	Full Scale	Primary factors contributing to performance: Heat Pump machine, circulating Pump, and ground coupling,
[3]	N/A	Variable Refrigerant Flow vs. GSHPs	N/A	R410A Refrigerant	Simulations only	Computer - EnergyPro analysis and DOE-2.1	Full Scale	GSHPs are more energy efficient
[4]	Ege University, Izmir, Turkey	Performance Evaluation of GSHPs - Basic COPs	Solar Assisted Vertical vs. Horizontal, Both Closed	R22 Refrigerant	Full Scale designed to heat a test room of 10 sq meters in Turkey	Analytical Modeling	Full Scale	Solar Assisted COP = 3.64 Horizontal Cop = 3.43
[5]	University of Firat, Elazig, Turkey	Numerical Model and Experimental Analysis of Horizontal Ground Coupled Heat Pump	Horizontal Closed U-loop	Water - Antifreeze Solution	Full Scale designed for a test room	Computational Modeling was used. Meshes created for the ground region of the room, for temperature distribution data	Full Scale	Avg Cop = 3.2 and numerical results matched experimental after some changes were made
[6]	Tokyo, Japan	Predicting the Heat Exchange Rates of a GSHP	Vertical Closed U-loop	Water	Full Scale designed for an Office Building in Japan	Computational Modeling was used. Meshes created for the cement region, where U-tube was	Full Scale	Simulation/Computational Modeling was successful in predicting the exchange rates.
[7]	Oklahoma University	New Method to Determine Thermal Properties of the Soil from In Situ Field Tests	Vertical Closed U-loop	N/A	Full Scale at Two Elementary Schools and a test rig at Oklahoma University	Mostly analytical	Full Scale	Test Rig results were consistent with analytical prediction after 30 hrs overall less than 5% error

Esen et al. (2007) performed numerical modeling on a horizontal closed U-loop to determine the coefficient of performance (COP). The numerical results matched that of the experimental results, with an average COP of 3.2 during the heating season. The numerical modeling was used to determine temperature distribution of the test site. The site was modeled as a two dimensional non steady heat conduction problem. Several assumptions were made in order to model the site footprint in this manner: convection and radiation are negligible in the soil, moisture migration is ignored, ground properties are uniform, ground temperature only varies seasonally, symmetric heat transfer, the distance between loops is large enough to avoid thermal interference, heat transfer parallel to the pipes is negligible, and gravity, rainfall and snowfall effects are negligible. The experimental model was a horizontal U-loop installed at a depth of 1 meter and monitored with thermocouples. The interfaces between the earth and pipe, and the pipe and working fluid were also measured and monitored using T-type thermocouples resulting in temperatures used to determine COPs, which also matched the results of the experimental modeling.

Nam et al. (2008) devised a numerical model that combines a heat transfer model with ground water flow. Wet or damp soil has a greater thermal conductivity and the program FEFLOW uses finite element methods to model the heat exchange rate between the ground heat exchanger and the surrounding soil given a fluid motion. This program was used in their study

to do just that and the mesh for this simulation is shown in figure 3. The simulation results matched that of the experimental test, proving soil temperatures are higher due to fluid flow through the soil. The simulation was confirmed through tests conducted on an office building in Tokyo. In the office building a set of 8 U-loops was installed to a depth of 20 m and monitored while the ground water flow was modeled around the pipes at a depth of 12 m. As stated above, results from this “real world” study confirmed that fluid flow increases soil temperature. Additional cases, where the number of U-loops varied, were also studied and it was seen that with more pairs of U-loops the COP was greater.

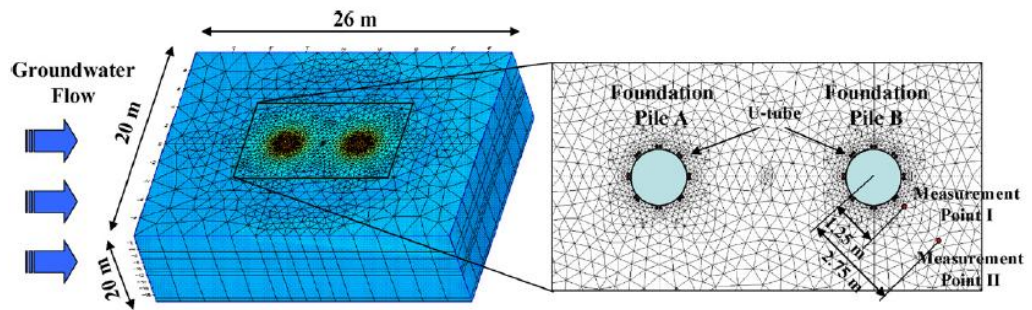


Figure 3- Mesh of Simulation Model for a U-loop pair (Nam et al, 2008)

Hepbasli et al. (2001) found the heat extraction rate from the soil to a borehole at a depth of 50 m was on average 11W/m of bore depth using passive solar techniques. The soil had a thermal diffusivity of 0.00375 m²/h and the entering water temperature ranged from 5.5 to 13.2 °C. The authors discussed in great detail the importance of each part of the GSHP, from determining the soil characteristics, to the efficiency on the pump and how each factor affects the heat exchange rate. Soil type, temperature and

moisture gradients are some of the most influential factors for heat exchange from the soil to the working fluid. The thermal diffusivity and conductivity of soil are just two examples of important parameters determined and affected by the three characteristics listed above. The overall efficiency of the GSHP is influenced by three main factors: the heat pump machine, the circulating pump and ground coupling. It was determined that performance could be improved by adjusting a number of factors such as; minimize pipe friction, pumps should be selected to operate within 5% of maximum efficiency, reduce head losses, and limit the amount of antifreeze solution used, just to name a few.

Each of these articles gave insight into how to design the study discussed in this paper. A finite element analysis was planned to model heat transfer rates from the soil to the working fluid inspired by Nam's et al (2008) use of numerical modeling for ground water flow. Their positive results shed light on the effectiveness of this type of analysis. Several of the boundary conditions and assumptions made by Esen et al. (2007) were considered for this study or were stimulation for the assumptions made in this study. The importance of material parameters was driven by Hepbasli et al. (2001) and the discussion of soil parameters and how each element of the system affects the overall efficiency.

The ultimate goal of the current study was to model performance data, such as heat transfer rates, from different horizontal layouts. Using ANSYS

Fluent, a finite element study was completed for a U-loop, coil, and slinky coil, however only two were actually tested in this study, the U-loop and the coil. The goal was to determine if the shape of the layout affects the heat transfer rates of the system. The layout determined to be the most efficient was constructed, tested and compared to the computer modeled system. The remainder of this report discusses the methods used in the finite element study, the methods of verifying the ANSYS simulations and the results pertaining to each of the layouts, as well as the experimental tests conducted and how they compared to the simulations.

Chapter 2: Computational Fluid Dynamic Verification Studies

One must be careful when using finite element computer simulations. Typical pitfalls are improper meshing, lack of grid independence, or incorrect boundary conditions, along with a multitude of other parameters that could be set incorrectly. In order to avoid such complications and mistakes with the computational model, verification studies were devised and completed to check if the simulations were producing accurate results. This chapter presents two verification methods that were designed to compare the simulation results to a known analytical solution; shape factor and energy balance studies were used for verification.

To begin any simulation the layout was constructed using Solidworks 2010 (Educational Edition) and imported into ANSYS version 12.0.1 (Educational Edition) where meshing, boundary conditions and other parameters, such as materials, were set to the model and the simulation was then ready to be run. The test model can be seen in figure 4. The test model was a cuboid of 0.1m and had a cylindrical cut-out through the center with a diameter of 0.02m. This test model replicated a geometry for which the shape factor is known.

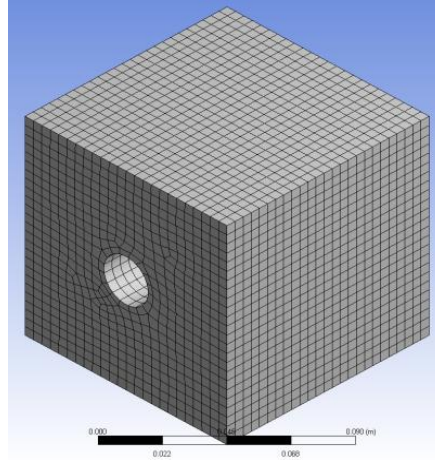


Figure 4 – Test Cube Model used for Verification Studies Showing Mesh

Shape Factor Verification

To conduct the shape factor verification the test cube, shown in figure 4 was constructed and imported to ANSYS. The solution was checked analytically using a shape factor for a known length of pipe submerged in a course medium, shown in equation 1, taken from table 4.1 of Incropera's *Introduction to Heat Transfer*.

$$S = \frac{2\pi L}{\ln(1.08 \frac{w}{D})} \quad \text{Eq (1)}$$

The boundary conditions were set as shown in figure 5. A temperature boundary was set to all four faces of the cube, excluding the inlet and outlet, and a temperature was set to the inner face of the soil where the cutout of the pipe was. The boundary condition values can be seen in table 2. The Solidworks model did not include the pipe material or fluid because the shape factor was simply the soil with a cylinder cut from the center. Replicating the

shape factor boundary conditions on the model in ANSYS produced comparable results to those calculated analytically and results for diameters of 0.01m and 0.02m can be seen in tables 3 and 4 respectively. These results were computed with varying conductivities (K , W/mK) of the soil, as well as different diameters of piping.

Where L is depth, w is width of medium, and D is diameter of the pipe

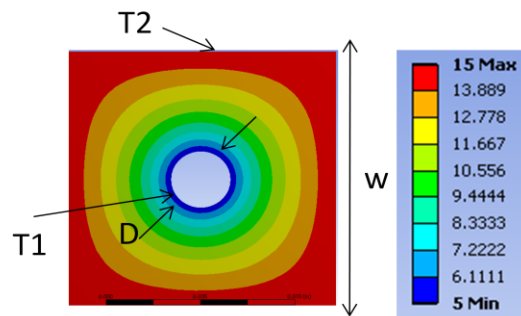


Figure 5 –Boundary Conditions and Temperature Distribution for Shape Factor

Parameters of shape factor: $K = 0.069 \text{ W/mK}$ and $D = 0.02 \text{ m}$

Table 2 – Shape Factor Boundary Condition Values

Condition	Value
T1 (C)	5
T2 (C)	15
W (m)	0.1
D (m)	0.01 and 0.02

Table 3 - Shape Factor vs. Simulation Results with a diameter of 0.01m

Diameter = 0.01m	Shape Factor (W)			
K value (W/mK)	Equation 1	Analysis	Eq1-Analysis	%Error
0.02	0.05278	0.05284	0.00006	0.107
0.05	0.13196	0.13210	0.00014	0.107
0.069	0.18210	0.18230	0.00020	0.108
0.1	0.26392	0.26420	0.00028	0.107
0.5	1.31958	1.32100	0.00142	0.107

Table 4 - Shape Factor vs. Simulation Results with a diameter of 0.02m

Diameter = 0.02m	Shape Factor (W)			
K value (W/mK)	Equation 1	Analysis	Eq1-Analysis	%Error
0.02	0.07448	0.07904	0.00456	6.12
0.05	0.18620	0.19760	0.01140	6.12
0.069	0.25695	0.27269	0.01574	6.12
0.1	0.37239	0.39520	0.02281	6.12
0.5	1.86196	1.97600	0.11404	6.12

It was found that the accuracy of the simulation was dependent on diameter size, shown in figures 6 and 7 for diameters 0.01m and 0.02m respectively. At the smaller diameter the error was small. The two lines representing the shape factor and simulation results agreed within 0.1% for the smaller diameter and within 6% for the larger diameter. During these test the mesh was kept constant for all the simulations and a finer mesh would have helped with the larger diameter. These results prove that the simulation was producing accurate results that are comparable to the analytical results.

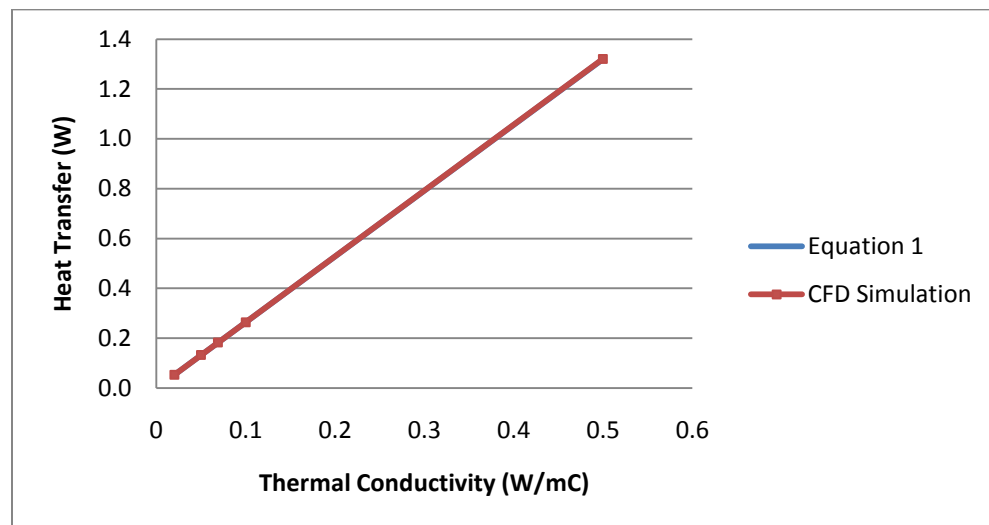


Figure 6 - Shape Factor vs. Simulation Results for a Diameter of 0.01m

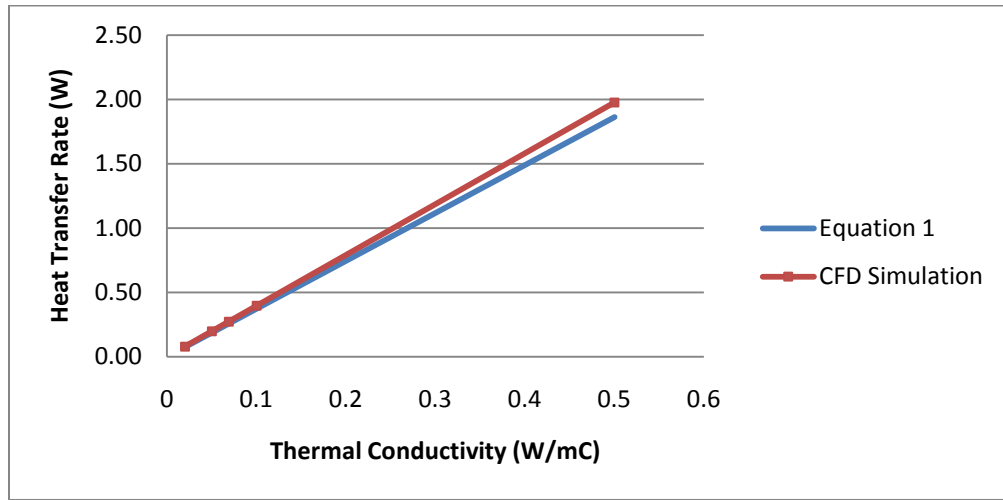


Figure 7 - Shape Factor vs. Simulation Results for a Diameter of 0.02m

Energy Balance Verification

Similarly, an energy balance was used as a second verification in ANSYS Fluent. The energy balance assured the heat into the system equaled the heat out. This cube, similar to the model shown in figure 4, included the layer of pipe and the fluid, unlike the shape factor which only included the soil. A known heat flux of 100W was set to all four faces of the cube, again, excluding the inlet face and outlet face. The test cube was 0.1m^3 , therefore 4 W of energy total were put into the system and the exiting energy was found to be 4 W from the ANSYS heat flux monitor results. This test was done on every layout that was made before simulations were completed.

The results and boundary conditions shown in figure 8 are from a U - loop energy balance verification simulation. Dimensions of the layout are shown in figure 8, as well and results are shown in table 5.

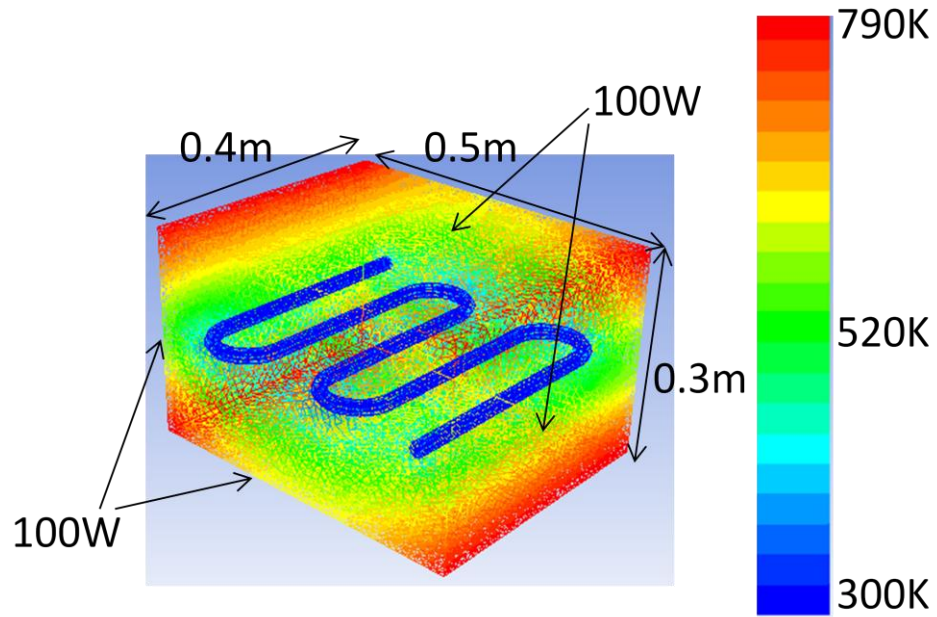


Figure 8 – U-loop Energy Balance and Boundary Conditions

Table 5 - Simulation Properties and Results

Properties	Value
V(m/s)	1
(kg/s)	0.28672
Cp (J/kgK)	2415
T _{in} (K)	300
T _{out} (K)	300.09
Q _{tot} (W)	63.99

Below are the steps used to calculate the total energy of the system when 100W was applied to each of the faces of the U-loop layout. This was a check that the energy into the system was equal to the energy leaving the system. The area of the face was calculated and then multiplied by the heat flux applied and all four sides were then totaled.

$$\begin{aligned}
100\text{W} (0.4\text{m} * 0.5\text{m}) &= 20\text{W} \\
100\text{W} (0.4\text{m} * 0.5\text{m}) &= 20\text{W} \\
100\text{W} (0.4\text{m} * 0.3\text{m}) &= 12\text{W} \\
100\text{W} (0.4\text{m} * 0.3\text{m}) &= 12\text{W} \\
&+ \frac{\quad}{64\text{W}}
\end{aligned}$$

The simulation result, shown in table 5, were used in conjunction with equation 2 to calculate the total heat transfer, which was found to be 64W. The results matched that of the simulation and area driven calculations shown above. Energy balances were achieved on both the test cube and the U-loop layout.

$$Q = \dot{m}C_p(T_{out} - T_{in}) \quad \text{Eq (2)}$$

Where \dot{m} is mass flow rate in kg/s, C_p is the specific heat in J/kgK, and T is temperature of the inlet and outlet

This chapter discussed two verification methods for the ANSYS simulations. These, as previously mentioned, were used to validate the accuracy of the simulations by comparing the results to an analytical solution method. The shape factor verification showed the accuracy to be around 6% and an energy balance was executed which agreed within 0.01% to the theoretical value on the simulations conducted for this study.

Chapter 3: Layout Studies

Results and discussion of the layout simulations completed and details about the simulation set up are included in this chapter, along with information about research done on simulation parameters, the materials used and their properties. Results for the U-loop, coil and slinky and subsequent conclusions are discussed below.

The ultimate goal was to isolate the layout from the remainder of the GSHP system to determine its individual contribution to the heat transfer. There were no external parts added to the simulations. Additionally, there were no other materials used that could possibly increase the heat transfer. A simple working fluid was used, one with a low or at least average conductivity and there was no grout applied between the soil and the pipe. In many installations grout could be applied to the inside of the borehole to enhance heat transfer from the soil to the working fluid. These “simple” materials were used to reduce external heat transfer and isolate the layouts as the main heat transfer factor.

Material Properties

Material properties were a large part of the research done for this study. The properties of the soil, piping, and working fluid affect the overall results for each layout. Research was done to determine what materials were typically used in the industry and at what temperatures and flow rates systems usually operate at.

Three layers were created for each layout model, the soil cube with the pipe layout hollowed out, the pipe made of high density polyethylene (HDPE) and the inner working fluid, ethylene glycol. The properties used can be seen in table 6. These materials were chosen because they are commonly used in industry. All these materials are standard issue in most geothermal systems were chosen because they were most likely produce realistic results.

Table 6 - Material Properties (Ground)

Property (268K)	Ethylene Glycol	HDPE	Loamy - Sand
Thermal Conductivity (K, W/m-K)	0.24	0.46	0.069
Density (ρ , Kg/m ³)	1135	950	1350
Specific Heat (Cp, J/kg-K)	2100	1800	800
Viscosity (μ , Kg/m-s)	0.054	-	-

The HDPE and ethylene glycol had known parameters and were found online and from previously tabulated texts. The properties for ethylene glycol (100%) were specified at the inlet temperature of 268K or -5°C. However, it was much harder to determine properties for the soil due to its varied nature. Access to the types of soil tests used to determine density, conductivity and other parameters were not available for this project and other methods for determining these properties were utilized.

The Web Soil Survey was used to determine the type of soil at Union College, specifically around the Nott Memorial. It was determined that the soil was loamy fine sand. A table of approximate conductivities for different types of soils, shown in table 7, was used to take an average of the two soil

types. The conductivity was determined to be 0.069 W/m-K, also shown in table 6. The conductivities of the soil will be varied to determine the effect of conductivity on the total heat transfer.

Table 7 - Thermal Conductivities of Soil (Ground)

Texture Class	Thermal Conductivity (BTU/ft hrF)
Sand	0.44
Clay	0.64
Loam	0.52
Saturated Sand	1.44
Saturated Silt or Clay	0.96

Layouts

Three layouts were researched in this study: the U-loop, coil and slinky. These three layouts were chosen because they are typically used in horizontal systems. The U-loop, coil and slinky can be seen in figures 9, 10 and 11, respectively. The U-loop and the coil were the only layouts simulated. The slinky was not tested due to geometric meshing challenges which will be discussed further later in this report. Further details about the U-loop and coil geometries and simulation results are contained in the subsequent sections.



Figure 9 – U-loop



Figure 10 – Coil



Figure 11 - Slinky

U-Loop Simulation

The U-loop simulation began with the layout in Solidworks. The dimensions of the soil were 1.03 m in depth, 0.4m x 0.5m wide. The layer of piping was dimensioned at a depth of 1 m to simulate the typical depth at which the ambient earth temperature of 15°C can be reached. The total length of the U-loop was 2.088m including elbows and each straight section of pipe was about 0.3m each. The diameter of the pipe was 0.02m or $\frac{3}{4}$ inch. These dimensions can be seen in figure 12 and 13. Overall, the dimensions of the layout are typical heights and diameters of geothermal systems.

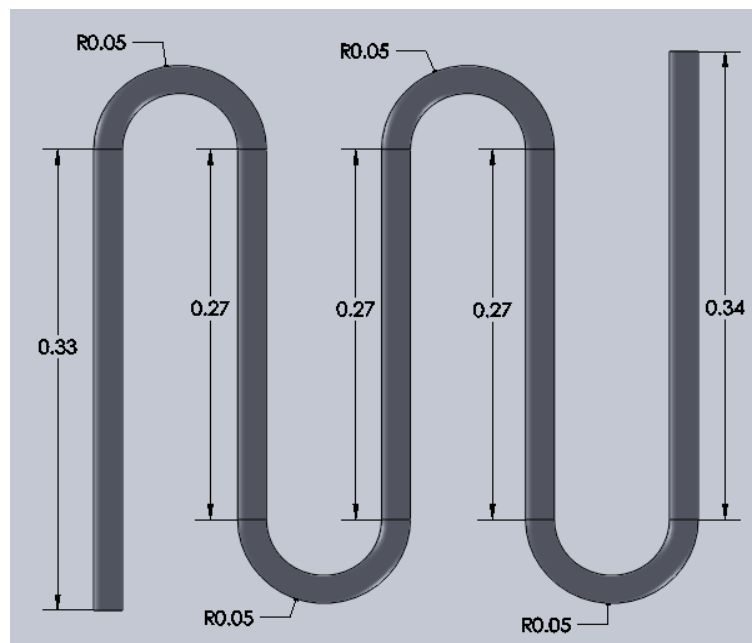


Figure 12 – U-loop Dimensions

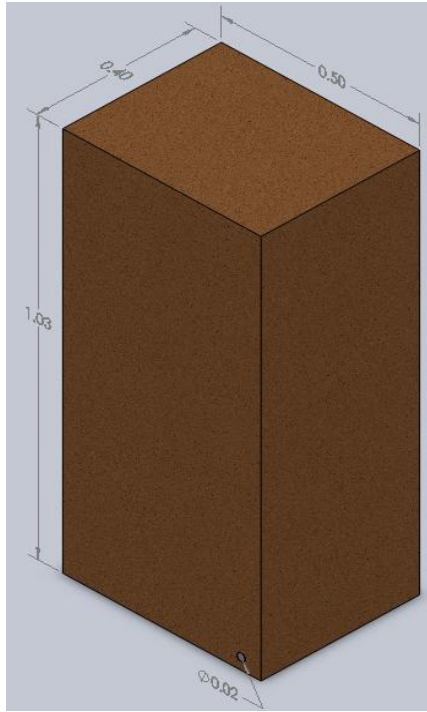


Figure 13 – U-loop Soil Plot Dimensions

The total length of the pipe for this study was much shorter than a typical system, and was only a small snap-shot of a system. Horizontal layouts are usually 100-150 m of piping and a system of this size can produce up to 10,000 W of energy. A system of this size on average produces 66 W/m in an infinite soil medium, which was not fully simulated in this study (Consumer, 2006).

The U-loop simulation was run at steady state, for laminar flow, with a velocity of 1m/s which corresponds to a flow rate of 5 gal/min. The Reynolds's Number for this flow rate was calculated to be 420 using ethylene glycol at 268K, which classifies as laminar. Velocities up to 5 m/s were all classified as laminar flows (see table 8). Equation 3 was used to calculate Reynolds'

Number for each velocity and properties used in the calculation can be seen in table 9 and the flow classification parameters are shown in table 10.

$$Re = \frac{\rho V D}{\mu} \quad \text{Eq (3)}$$

Where ρ is density of the fluid, V is velocity in m/s, D diameter which is the characteristic length, and μ viscosity of the fluid

Table 8 – Reynolds's Number Classifications

Velocity (m/s)	Re	Classification
1	420	Laminar
2	840	Laminar
3	1261	Laminar
4	1681	Laminar
5	2101	Laminar
10	4203	Turbulent

Table 9 – Simulation Properties

Properties	Value
V(m/s)	1
(kg/s)	0.358
Cp (J/kgK)	2100
A(m ²)	0.000314
K (W/mK)	0.24
D (m)	0.02
Viscosity(μ , kg/ms)	0.054
Density (kg/m ³)	1135

Table 10 – Flow Classification

Reynolds's Number	Classification
$Re \leq 2300$	Laminar
$2300 \leq Re \leq 4000$	Transitional
$Re \geq 4000$	Turbulent

The boundary conditions set for this layout were temperature and symmetry walls, a pressure outlet, velocity inlet, coupled interfaces and a thin wall shell conduction, which can all be seen in figure 14 and are also outline in Appendix B by the simulation report provided by ANSYS. The top temperature, 278K, was the ambient air temperature and the bottom temperature, 288K, was the ambient soil temperature. The interfaces were set on the inner soil and outer fluid. This interface tells the program that two different materials are touching and are thermally coupled. As previously mentioned, the piping was not physically modeled in the layout, but the thin wall shell conduction allowed a thickness of a specific material to be set between the interface sections, so the pipe was not physically there but was still thermally modeled. To simulate an infinite width of soil symmetry boundaries were set to both the left and right sides of the system.

The inlet and outlet boundaries were important, but the pressure outlet boundary was especially significant. If the outlet was set as an outflow the program would not converge because energy was not able to escape the system; the internal temperature just increased with each simulation. The pressure outlet however, allowed the program to converge and produce accurate results.

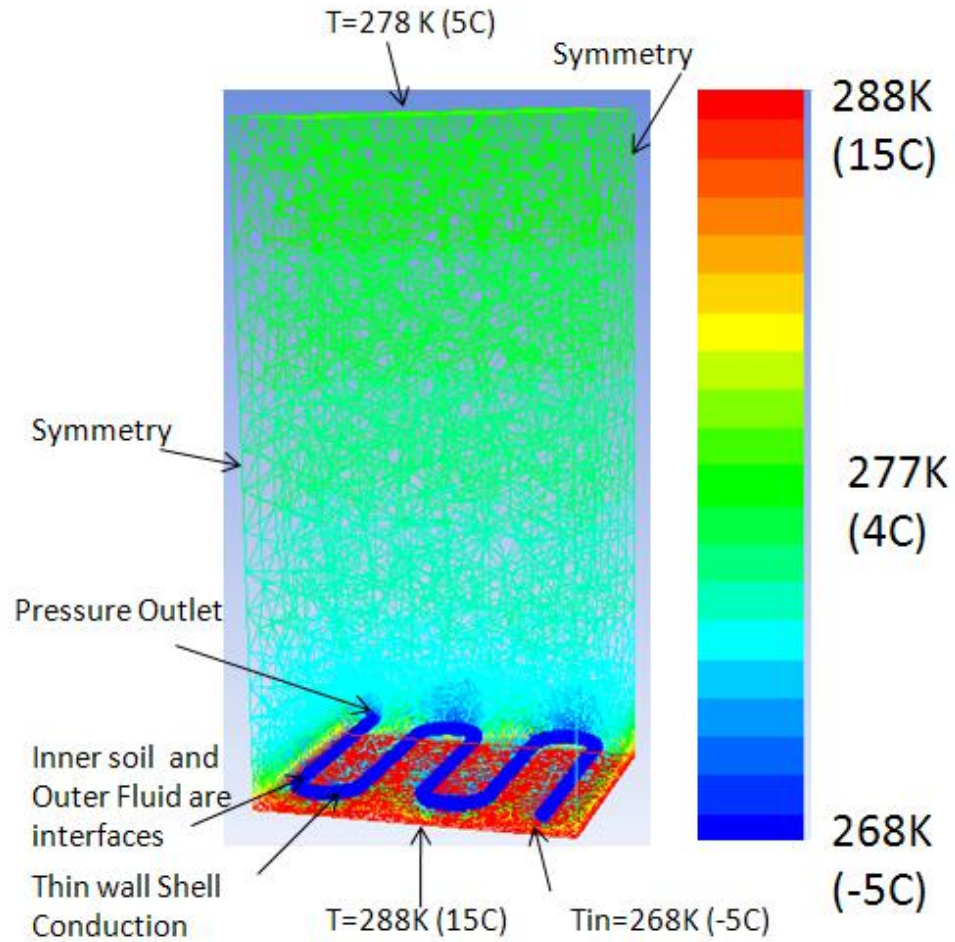


Figure 14 – Boundary Conditions and Temperature Distribution Results for U-loop Steady State Simulation

Steady State Simulation Results

Figure 14 shows the temperature distribution results from the laminar, steady state simulation of the U-loop which was run with an inlet velocity of 1m/s ($Re=420$) and an initial working fluid temperature of 268K. Further results can be seen in table 11. The steady state heat transfer was determined to be 7.5 W. This was the heat transfer calculated by the energy balance using equation 2, which was calculated to also be 7.5W. A transient

study was completed on the same layout to determine what was happening over time before the steady state heat transfer value was reached.

Table 11 – U-loop Simulation Input Properties

Properties	Value
V(m/s)	1
(kg/s)	0.3507
Cp (J/kgK)	2100
A(m ²)	0.000309

Transient Simulation Results

Two main transient studies were completed on all of the layouts; one with the initial condition of the inlet temperature of the fluid and the soil to be 268K and the second with the initial condition of the soil at 288K and the inlet temperature of the fluid at 268K. It was determined that the transient solution greatly depended on the initial condition of the whole soil body.

The graph shown in figure 15 displays the results of the first method of the transient U-Loop simulation where the initial condition of the fluid was set to 268K. The interface boundary conditions were monitored for the total heat flux on the surface over time. It can be seen that the outer fluid's heat transfer increased and the inner soil decreased over time. This essentially means that the temperature of the fluid increased because it was extracting heat from the soil, thus the soil temperature decreased.

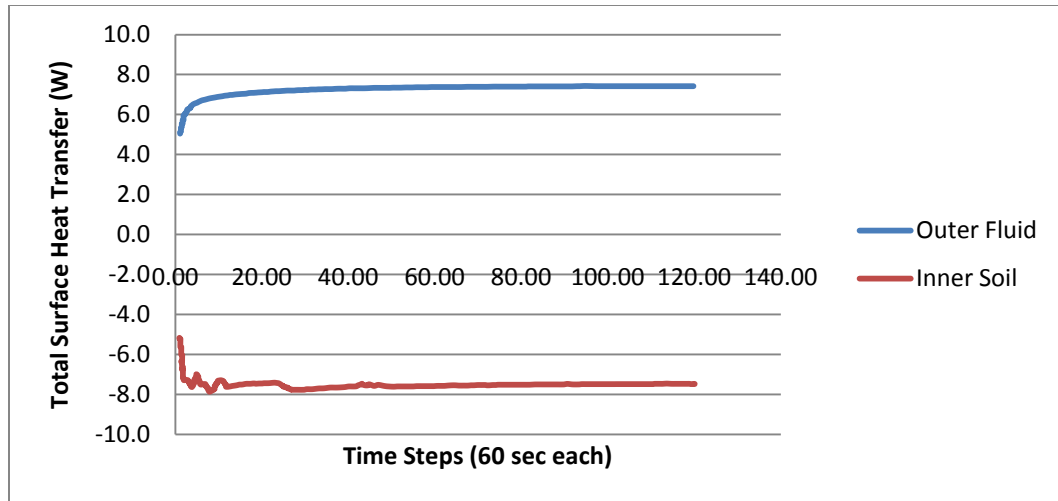


Figure 15 – U-Loop Heat Transfer from the First Method Transient Solution

These results show that the heat transfer between the soil and the working fluid was even. The soil was directly transferring the heat to the working fluid. The graph in figure 16 shows the second transient solution where the initial temperature of the fluid is 268K and the initial temperature of the soil was 288K.

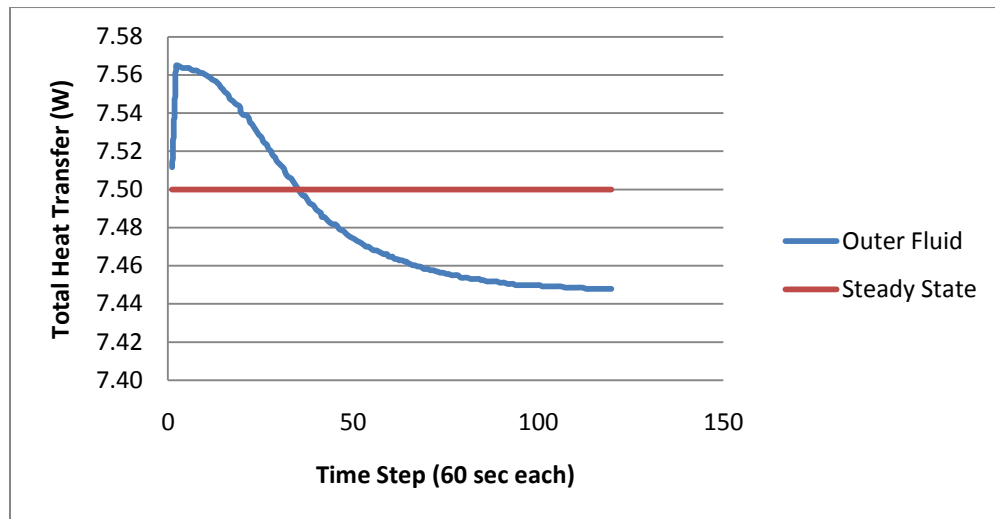


Figure 16 – U-Loop Heat Transfer Results from the Second Method Transient Solution

The secondary method for the transient solution uses a patch during the initialization of the simulation. This patch allows different initial temperature conditions to be set for different sections of the model. With these conditions the heat transfer of the outer fluid follows the predicted pattern of a larger heat transfer initially and a gradual decrease as the temperature difference between the soil and the fluid reaches the steady state value around 7.5 W.

Coil Simulation

The coil model, just as the U-loop was created in Solidworks. The dimensions of the outer soil were set as 0.50m x 0.45m x 1.03m. The coil was approximately 2.1 m long. This was equivalent to the length of the U-loop configuration. The diameter of the pipe was again, 0.02m or $\frac{3}{4}$ of an inch. The only parameter that varied between the two layouts was the configuration of the same length of piping. The configuration and soil dimensions can be seen in figures 17 and 18.

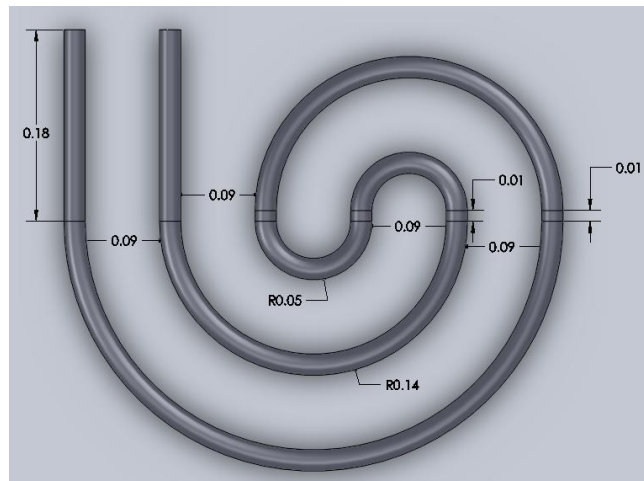


Figure 17- Coil Dimensions

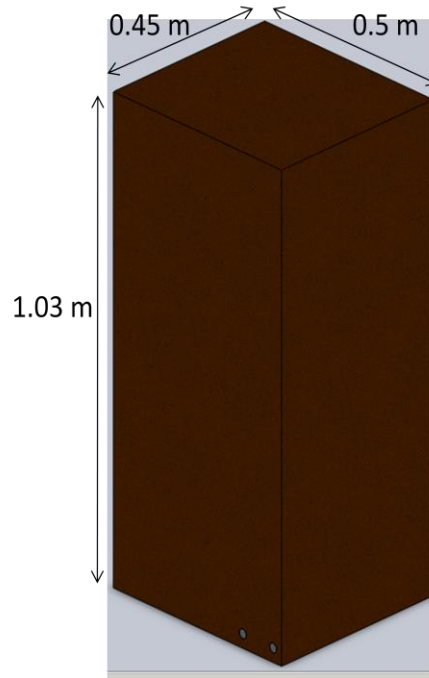


Figure 18 – Coil Soil Dimensions

Steady State Simulation Results

The steady state simulation produced a heat transfer of 8.3 W. This was run at a velocity of 1 m/s and an inlet temperature of the working fluid of 268K, just as in the U-loop simulation. The Reynolds's number was found to be 420 and the Reynolds's numbers for other velocities were shown previously in table 8. Again, all of the boundary conditions for the coil simulation were set to the same boundary conditions used in the U-loop simulation. The boundary conditions can be seen in figure 14 of the previous section.

A temperature distribution can be seen in figure 19 for the steady state simulation. This figure shows that the center of the soil was much cooler than the top or the bottom of the system. This was because the working fluid was drawing heat from the soil immediately around the coil and lowering the

overall temperature. The results of the steady state simulation can be seen in table 12.

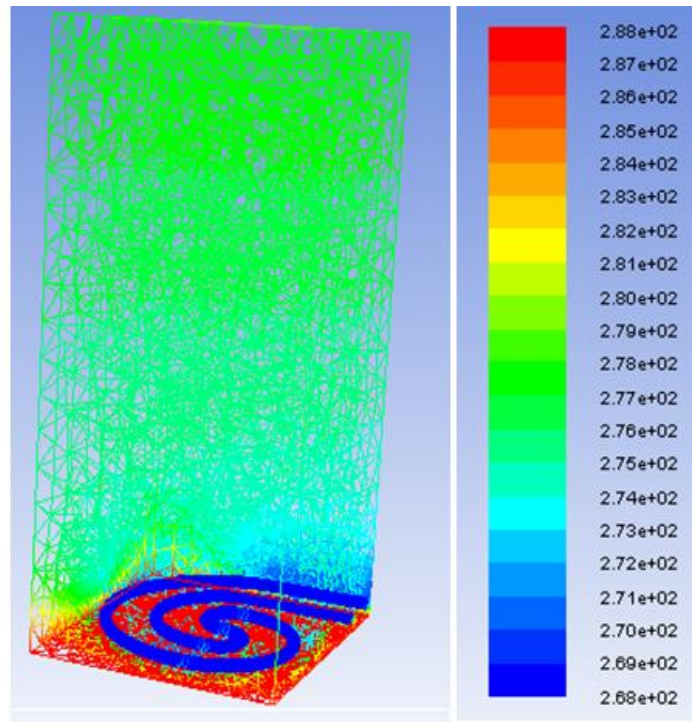


Figure 19 – Temperature Distribution Results for the Steady State Coil Simulation

Table 12 – Coil Simulation Input Properties

Properties	Value
V(m/s)	1
(kg/s)	0.3507
Cp (J/kgK)	2100
A(m ²)	0.000309

Transient Simulation Results

Two transient solutions were conducted, as explained previously, changing the initial temperature condition of the soil. As in the U-loop simulation the heat transfer between the two interfaces, fluid and soil, was

monitored during the first method for transient simulation, and the results can be seen in figure 20. The initial condition of the soil for this simulation was 268 K. This simulation was run for 2 hours in 120 time steps which were 60 seconds each.

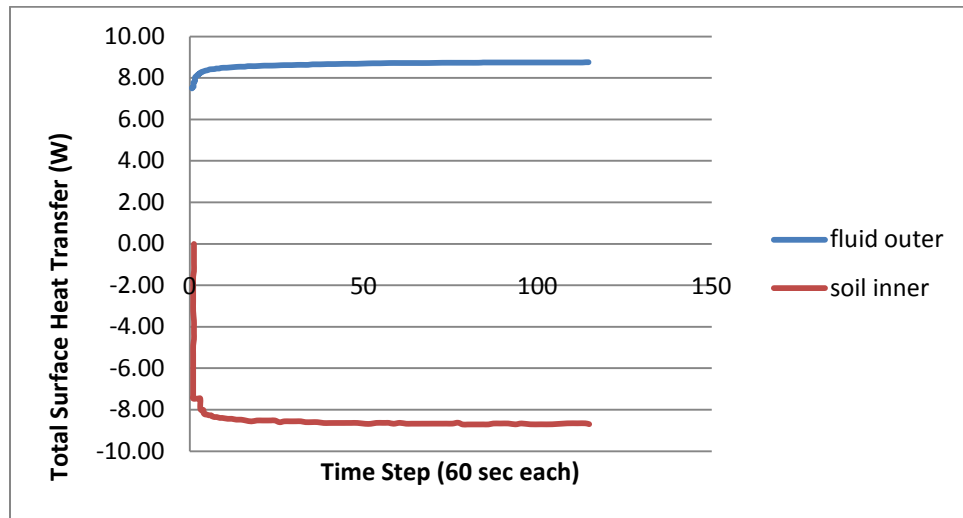


Figure 20 – Coil Heat Transfer for the First Method Transient Solution

The results were very similar to those of the U-loop. It was seen that the soil heat transfer decreased and the fluid heat transfer increased. The first method's results were mainly based on the initial temperature condition of the soil as a whole. The second transient method was then simulated. The initial condition of the soil body was set to 288K and the fluid's initial condition was patched at 268K. The results of the second method can be seen in figure 21.

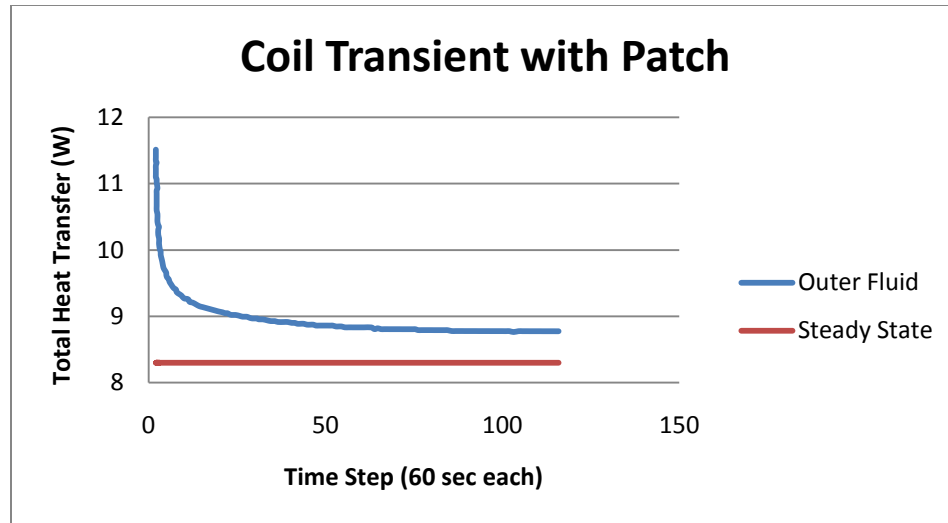


Figure 21 – Coil Heat Transfer from the Secondary Method Transient Solution Simulation

Figure 21 shows that the heat transfer decreased rapidly in the first few time steps and continue to decrease until the system approached steady state. This system almost reached the steady state value, 8.3W, determined by the steady state simulation. If the simulation was run for more time steps the full steady state value would have been reached.

Slinky Simulation

The slinky shape was constructed and imported into ANSYS for simulation; however there was an error with the interfacing that could not be resolved within the time frame of this project. Results were obtained from the other two layout simulations, so this layout was not considered necessary at this time. The shape of the slinky coil can be seen in figure 22. This shape, like the other layouts, has a length of 2.1m and was surrounded by the block of soil with the same dimensions listed for the coil layout. Results from the slinky layout were not used in this study.

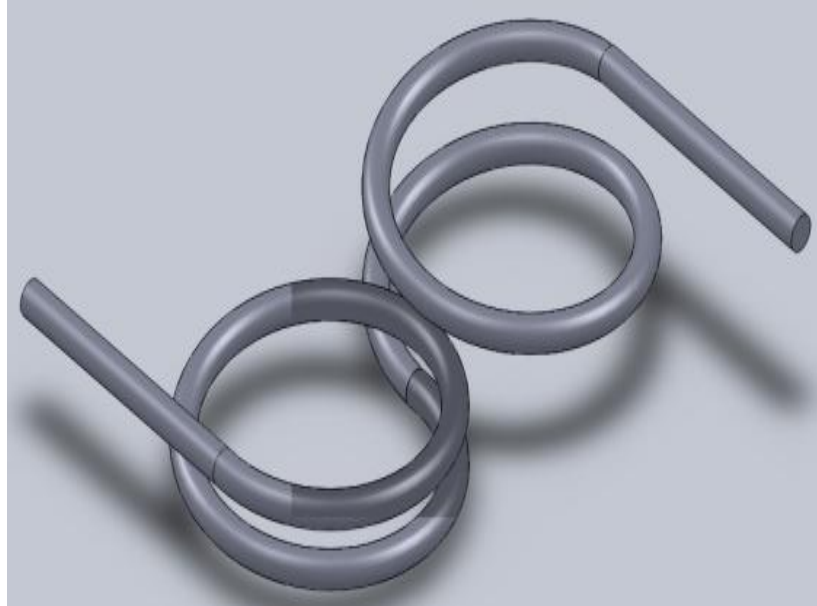


Figure 22 – Slinky Coil Layout

Comparing the two systems, U-loop and coil, it can be seen that the coil produced more overall heat transfer, once steady state was reached. The U-loop produced 7.5 W and the coil produced 8.3W. This proves that the layout does make a difference. It was believed that the proximity of the coils may have had an effect on the total heat transfer in the soil layout, shown in figure 23; if the coils are closer then there may be some carry-over heating through the soil to the adjacent coil.

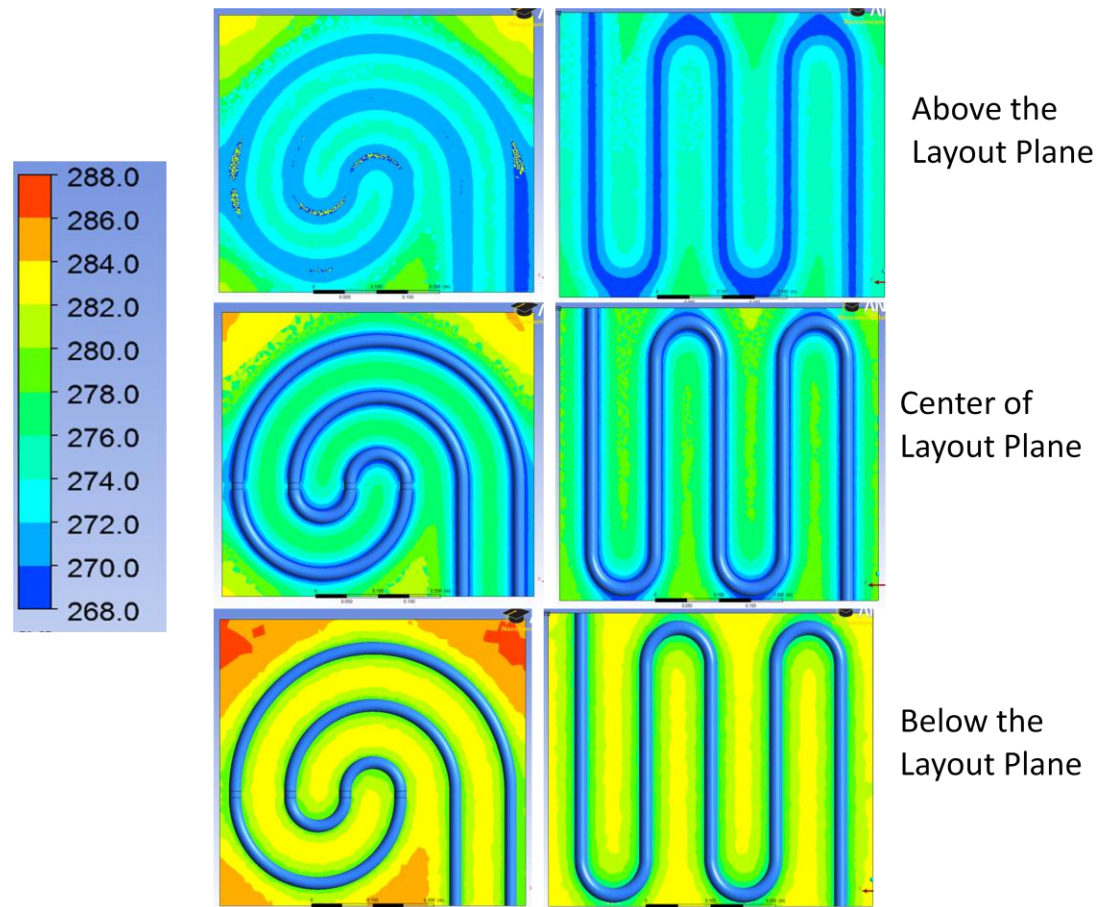


Figure 23 – Temperature Distribution Comparison between the Coil and U-loop on Three Different Planes

In figure 23 it can be seen that carry-over heating is a plausible explanation for the difference in the steady state heat transfer values of the two layouts. In the center plane for the coil, segments of soil are at a higher temperature mainly in the upper corners. This type of significant temperature difference is not seen on the center plane of the U-loop. Moreover, moving to a plane slightly below the height of the layout, it is seen that the coil again, has a significantly higher temperature in some sections. Also looking at the temperature of the soil adjacent to the piping, the soil around the coil layout is at a higher temperature than that of the U-loop.

As stated in the previous section the typical length for a horizontal system is 100-150 m and it should be reiterated that this system was not to scale. The results from the steady state tests, for both the coil and U-loop, are the heat transfer once the system reaches steady state. This result was used to compare the systems because it was a known measurable parameter in all of the simulations.

Chapter 4: Experimental Model

An experimental model of the heat pump layout was constructed to test the most thermally efficient system. This system was determined by comparing the heat transfer rates from the steady state simulations of both the U-loop and the coil layouts. The coil simulation produced 8.3 W and the U-loop produced the 7.5W. The coil layout was constructed and experimentally tested because it had the higher steady state heat transfer.

Test Apparatus

The experimental apparatus design was slightly altered from the original shape used in the ANSYS simulations. The soil block was shortened, and the inlet and outlet were centered in the height of the box, instead of being located lower on the box. This was done to make the size of the test apparatus more manageable. The design can be seen below in figure 24.

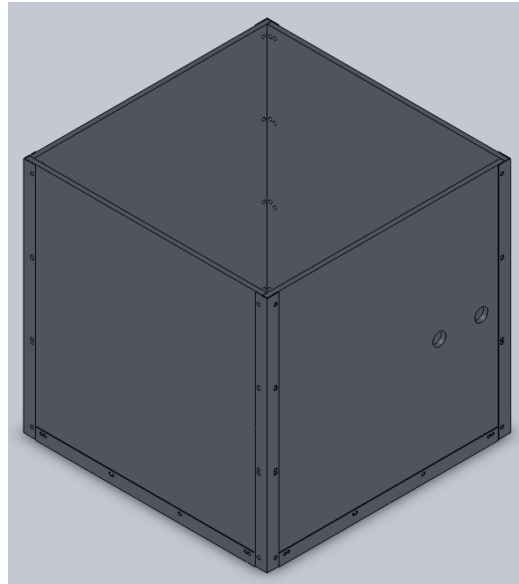


Figure 24 – Solidworks Drawing of the Experimental Test Apparatus

The test apparatus was given dimensions 0.5m x 0.5 x 0.5m. It was reinforced with corner angles to ensure that the structural integrity would be maintained once the heavy soil was added. The material used for the siding of the cube was Lexan plastic. This material was chosen because it would insulate the system more or at least prevent a great loss of heat during testing, and it was easier to machine than Plexiglas. Tygon tubing was selected to simulate the high density polyethylene (HDPE) tubing that is usually used in larger ground source heat pump systems. The HDPE has a very large bend radius and would not be suitable for a project of this scale. The finished product can be seen below in figure 25.



Figure 25 – Finished Experimental Test Apparatus

This test unit was filled with moist soil to simulate the condition of the soil underground. The soil was also left to compact under its own weight. No further packing was done as to simulate natural conditions. Densely packed soil is more conductive than loose soil because it has fewer air voids and this

could have enhanced heat transfer, possibly skewing data referring to the layout shape.

The working fluid was water mixed with ZECOL, RV Plus Antifreeze, whose main ingredient is propylene glycol which has similar properties to ethylene glycol, but is non – toxic and much safer to work with. A Utilitech 1/6 HP utility centrifugal submersible pump was used to circulate the working fluid through the system.

A fish tank heater was placed in the water to control the working fluid temperature. It was decided that the fluid would be heated because heating the soil and maintaining a constant temperature would have been too difficult. Since the working fluid was heated, a reverse geothermal procedure would happen; the working fluid would heat the soil instead of the soil heating the working fluid. This, in turn, meant that the working fluid needed to be heated above the temperature of the soil.

Thermocouples were placed in the soil to monitor the temperature as the working fluid flowed through the system. As previously stated, the working fluid would increase the temperature of the soil decreasing its own temperature and the temperature difference between the inlet and the outlet was monitored, again using thermocouples.

Seven K-type thermocouples were placed in the apparatus. Three were placed in the soil, one in the center, one on the upper right corner and the other in the lower left corner. Two were placed at the inlet and outlet and

were positioned through the tubing to monitor the temperature as soon as it entered and exited the system. One thermocouple was also positioned in the water bath and another in the air. Figure 26 and 27 show a top and side view of the thermocouple positioning. In figure 26 thermocouples are also located at the inlet and outlet.

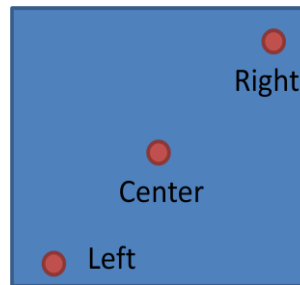


Figure 26 – Top View of Thermocouple Positions

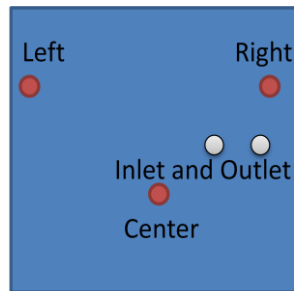


Figure 27 – Side View of Thermocouple Positions

The completed apparatus can be seen in figures 28, 29 and 30. Figure 28 is a schematic of the entire test apparatus set-up, figure 29 is the completed test apparatus unit, and figure 30 is the data acquisition system used to record the temperatures the thermocouples were monitoring and the pumping system along with the heating implement can be seen in figures 31 and 32.

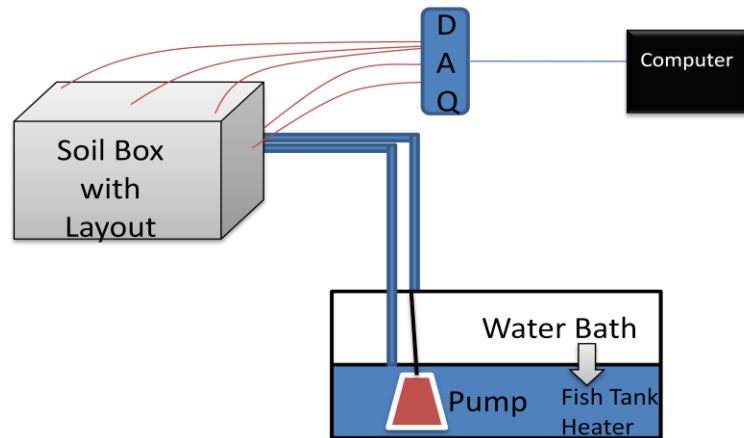


Figure 28 - Schematic of the Experimental Test Apparatus Setup



Figure 29 – Test Apparatus Unit



Figure 30 – Data Acquisition System and Digital Reader



Figure 31 – Test System Figure 32 – Pump and Heating Systems

Experimental Procedure

Three different experimental tests were run, two run with water as the working fluid and one run with antifreeze. Of the two run with water, one of the sets of data was collected over 3 hours using a DAQ View acquisition system and the other was run for $\frac{1}{2}$ hour and data was taken by hand with the digital reader. The third test, run with the antifreeze, was also a $\frac{1}{2}$ hour test and the data was taken by hand.

For each test the water was heated to 300K using the fish tank heater. The water was circulated every 5 minutes to ensure even heating, and it took about 20 minutes for the water to come to full temperature. The pump was only rated for temperatures up to 100F which is 310K, so the water was heated without the pump in the bath to ensure the safety of the user and the pump.

After the water had reached 300K the pump was placed in the water and the fish tank heater was removed. In initial testing it was seen that the

residual heat from the pump was able to keep the water bath at a constant temperature without the use of the fish tank heater for re-heating.

Once the pump was primed the data acquisition system was started and the pump was turned on. When using the digital reader the pump was started before data was taken. However in that situation, initial temperatures of all the thermocouples were recorded before the pump was started.

All of the thermocouples were monitored and the data was recorded, plotted and analyzed. Specifically, the temperature difference between the inlet and the outlet was monitored carefully and used to determine the amount of heat transfer in the system over the length of the test period. The heat transfer was calculated using equation 4 below.

$$Q = \dot{m}C_p\Delta T \quad \text{Eq (4)}$$

Where Q is heat transfer, \dot{m} is the mass flow rate (experimentally collected during initial pump testing), and C_p is the specific heat of the fluid.

Lastly, it should be noted that the system had to redistribute the heat gained during the test run and the temperature of the soil had to settle back to room temperature before another test could be run. Only one test was run per day and the system was left overnight to return to room temperature conditions.

Experimental Results

Two different sets of results are discussed below: the simulation results conducted in ANSYS and the experimental test results collected using the test apparatus. The simulation results were used as a prediction of the test results. Both sets of results will be discussed in the subsequent sections.

Experimental Computational Fluid Dynamic (CFD) Simulation Results

An experimental simulation was completed using ANSYS Fluent. The goal was to predict the outcome of the experimental tests by replicating the exact situation in ANSYS. A transient simulation was modeled and the original boundary conditions used in the other two simulations were modified. The initial temperature of the working fluid was changed to 300K and the initial temperature of the soil was set to 288K. This was done to simulate the heat transfer from the working fluid to the soil. A patch was used in the initialization to set the soil and working fluid to two separate conditions.

The transient graph shown in figure 33 displays a prediction of what the system should produce as a steady state heat transfer value, shown to be 2 W. These results were also used to predict the measureable temperature difference between the inlet and the outlet. The predicted temperature difference was about 1.5 degrees found using equation 4.

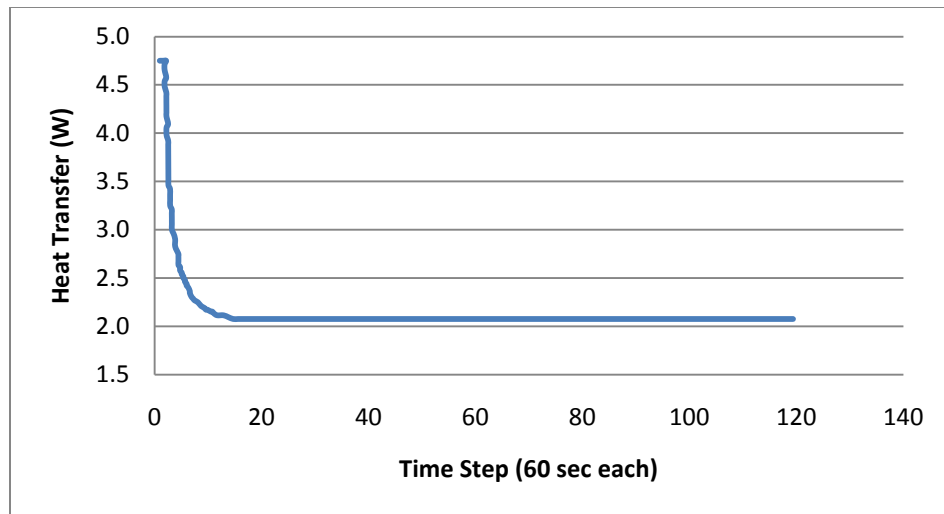


Figure 33 – Experimental Simulation Predicting the Heat Transfer of the Test Setup

Experimental Test Results

All three of the experimental tests were considered inconclusive.

There was no measurable heat transfer recorded from any of the tests. The accuracy of the thermocouples used to measure the temperature was ± 1 degree and because of this the overall results cannot be validated due to the very small temperature differences measured.

The water test where the data was collected using the DAQ view system produced no meaningful results due to significant noise in the system during the test. It is believed that the noise was increased when the pump was turned on. Submergible pumps can run a current through the water when pumping and this could have affected the accuracy of the thermocouple placed in the water and thus possibly affecting the other thermocouple connected through the same acquisition box.

To trouble-shoot this several things were done. A different acquisition box was used, the thermocouple was not placed in the water, and a different computer was used with a different operating system. None of these things solved the problem, there was still an excess of noise in the system, possibly still caused by the pump, and instead of using the DAQ view system the digital reader was used.

Water Test

The water test run for ½ hour was completed as a base case before the antifreeze was run through the system. The results from this can be seen in figure 34.

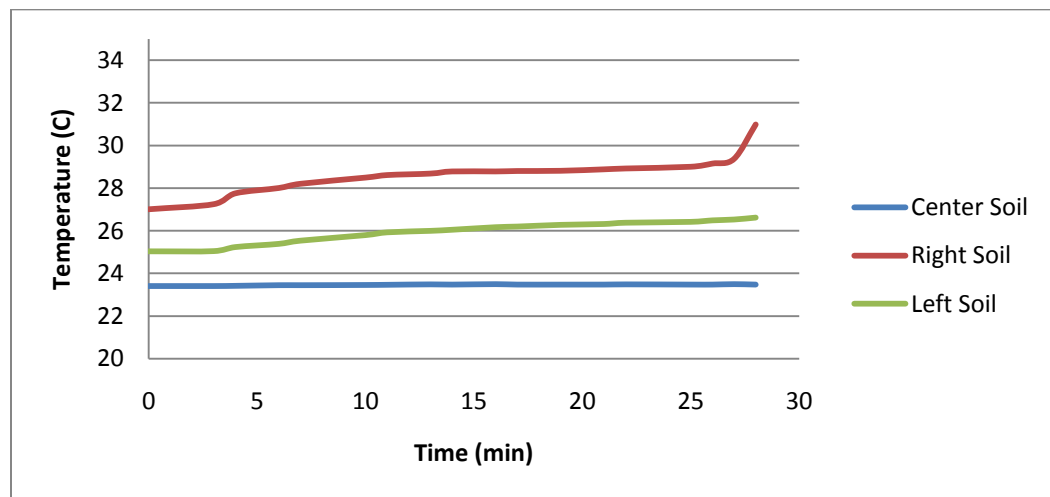


Figure 34 – Soil Temperatures from Experimental Test Run with Water

Figure 34 shows the increase in soil temperature during the half hour test run with water. An increase of about a degree was seen for the left and right sides of the soil and the center had no significant increase. These results bode well for the test with the antifreeze because the antifreeze has

better heat transfer properties a more significant increase in the soil temperature would be expected.

A trend was seen in the total heat transfer of the test run with water which was similar to the trend produced by the simulation shown in figure 33. However, the temperature difference which produced this trend was so small that this data was not reliable and was considered inconclusive. No appreciable heat transfer can be calculated with a temperature difference less than 1 degree.

Antifreeze Test

The test completed with the antifreeze produced greater temperature increases in the soil, and a heat transfer trend was still inconclusive. The soil temperature results can be seen in figures 35.

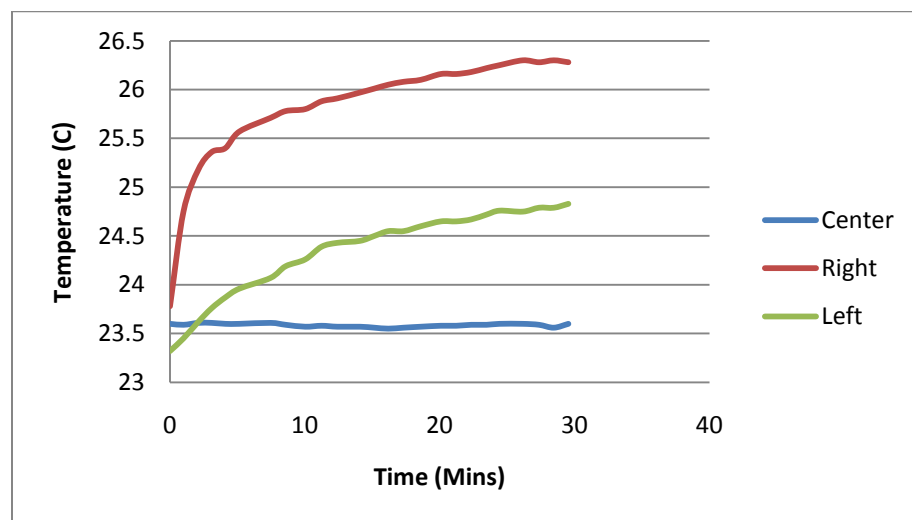


Figure 35 – Soil Temperatures from Experimental Test with Antifreeze.

A larger temperature increase was seen in the soil compared to the test run with water. Again the left and right sides' temperatures increased more

than the center soil's temperature. This was possibly due to rising heat, and the left and right probes were located higher in the test apparatus than the center, as shown by figure 27. Also, because the center thermocouple was located deeper in the apparatus it was not affected as much by the ambient room temperature.

There were no overall trends observed with the heat transfer of this test and the results are again inconclusive. There was less than 1W of heat transfer at any of the given time steps and this was directly related to the inlet and outlet temperatures. The difference between the inlet and the outlet was too small to calculate any appreciable heat transfer; the average temperature difference was about 0.2°C.

Experimental Conclusions

The experimental results were inconclusive however several things were learned. Many adjustments would be made to this experimental setup, along with several suggestions for future experimentation. In order for this experiment to yield successful measurable results a larger temperature difference must be achieved between the inlet and the outlet.

To achieve this type of temperature difference the water temperature could be increased and the flow rate could be reduced from 5 gpm to maybe 1 or 2 gpm. This test should also be done outside in the natural environment with real soil at a full scale depth. This would allow the length of tubing to be longer which would allow for a greater temperature difference. If a sizable

temperature difference can be measured then a more accurate assessment of the heat transfer could be calculated.

Chapter 5: Conclusions and Future Work

Conclusions

The main objective of this study was to determine if the shape of the layout affected the overall heat transfer of the system. It was shown that the U-loop layout produced 7.5W and the coil produced 8.3W, which is a 9.6% difference, thus the shape does seem to make a difference in the overall heat transfer.

This difference was attributed to a possible “carry over” heating that occurs between the tubes of the coil layout, shown in the temperature contour in figure 23. The soil space between the U-loop was greater than the soil space between the piping of the coil layout. If this system was scaled up the difference between the heat transfers of the two systems would increase significantly and the shape of the layout would be a larger factor in the efficiency of the system.

As stated in the introduction, “rules of thumb” are currently being used to make decisions about layout shapes in current system. These choices are mainly based on the amount of land available. This study took the same amount of land and the same length of piping in different shapes to prove that a greater overall heat transfer can be achieved. This could possibly help the industry make more efficient choices, ensuring the most optimal system.

Future Work

Further work that could be done on this project is vast. Other layout shapes could be tested, particularly the slinky shape. The slinky shape was

not analyzed in this study because the geometric issues within ANSYS were too complex to solve in the time allotted for this project. I think it would be interesting to see how this layout compared to the coil and U-loop and could see this project extended to accommodate those results.

Stemming from this project; the experimental setup could be tested with the suggested changes. This system would produce much more accurate results if it was tested at full scale or at least half scale of a real system. Other areas of the field that could be researched are the working fluids and how thermally efficient they are. Also grouts and backfill materials are being researched and tested for their ability to enhance the overall heat transfer from the soil to the working fluid. The geothermal industry is new and there is a lot of research that can be done to improve the current technology being used in the systems.

Works Cited

- [1] Armstead, Christopher. "Geothermal Energy." New York: E.&F.N. Spon, 2nd Ed. 1983
- [2] "Consumer Energy Center – Geothermal Heat Pumps," Copyright 2006 http://www.consumerenergycenter.org/home/heating_cooling/geothermal.htm
- [3] "Debunking Geothermal Myths," Bioengineering Group, Inc. Copyright 2010 <http://www.bioengineering.com/projects./renewableenergy/index.php>
- [4] Esen, Hikmet Inalli, Mustafa Esen, Mehmet. Numerical and experimental analysis of a horizontal ground-coupled heat pump system. Building and Environment 42 (2007) 1126-1134
- [5] "Geothermal, a product of Alliant Energy," <http://www.alliantenergygeothermal.com/HowItWorks/ClosedLoopSystems/index.htm>
- [6] "Ground Source Heat Pumps," Geo4VA. <http://www.geo4va.vt.edu/A1/A1.htm>
- [7] "Geothermal Technologies Program," US Department of Energy. <http://www1.eere.energy.gov/geothermal/history.html> last updated 11/01/2006
- [8] Incropera, Frank P. "The Conduction Shape Factor." *Introduction to Heat Transfer*. Hoboken, NJ: Wiley, 2007. 207-12. Print.
- [9] Nam, Yujin Ooka, Ryoza Hwang, Suckho. Development of a numerical model to predict heat exchanger rates for a ground –source heat pump system. Energy and Buildings 40 (2008) 2133-2140
- [10] "Natural Resources Canada," <http://oee.nrcan.gc.ca/publications/infosource/pub/home/heating-heat-pump/gsheatpumps.cfm> last updated 4/20/2009

Appendix A – Challenges

ANSYS presented several challenges as the test and layout simulations were being programmed. For instance, a major setback in the U-loop simulation occurred with the mesh. The educational edition of ANSYS limits the amount of cells per mesh and the part cannot exceed 512,000 cells. The U-loop layout was very large and with all three parts, soil, pipe and fluid, there were many surfaces that required meshing, which put the system over the educational limit.

Solutions to this problem manifested themselves as changes in the element size, which did not result in a successful mesh; changing minimum and maximum cell sizes, which allowed the parts to mesh, but resulted in a poor mesh quality which would lead to poor results. Ultimately, the pipe layer was removed and replaced with a thin wall shell conduction boundary condition. A growth rate was set as the meshing parameter, which allowed for a fine mesh around the fluid and for the cells to grow as they reached the outer limits of the part. It was acceptable to have larger cells near the edge of the part because less accuracy was needed farther from the fluid's path. A mesh constructed using a growth rate of 1.3 can be seen in figures 1 and 2.

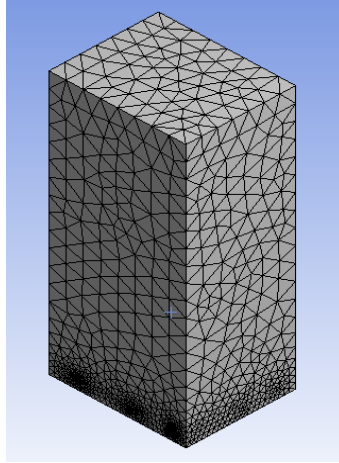


Figure 1 – Soil mesh using growth rate of 1.3

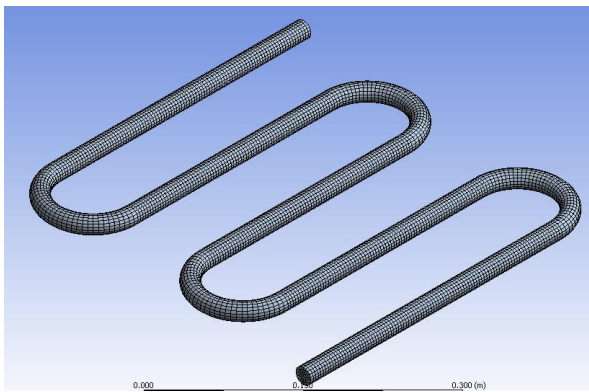


Figure 2 – Fluid Mesh using a growth rate of 1.3

A mesh dependency study is usually performed in most any finite element analysis; however one was not completed in this study due to the large part sizes and the educational cell limit. The parts being meshed are so large and bring the mesh to the program's limit, therefore it is assumed that mesh or grid independence was achieved in the simulations.

Appendix B – ANSYS Simulation Report

FLUENT

Version: 3d, pbns, lam (3d, pressure-based, laminar)

Release: 12.0.16

Title: Coil Steady State Simulation Report

Note: Same Boundary Conditions were used for the U-Loop Steady State Simulation

Models

Model	Settings

Space	3D
Time	Steady
Viscous	Laminar
Heat Transfer	Enabled
Solidification and Melting	Disabled
Radiation	None
Species Transport	Disabled
Coupled Dispersed Phase	Disabled
Pollutants	Disabled
Pollutants	Disabled
Soot	Disabled

Material Properties

Material: hdpe (solid)

Property	Units	Method	Value(s)

Density	kg/m3	constant	950
Cp (Specific Heat)	j/kg-k	constant	1800
Thermal Conductivity	w/m-k	constant	0.40000001

Material: loamy-soil (solid)

Property	Units	Method	Value(s)

Density	kg/m3	constant	1350
Cp (Specific Heat)	j/kg-k	constant	0.80000001
Thermal Conductivity	w/m-k	constant	0.07

Material: ethylene-glycol (fluid)

Property	Units	Method	Value(s)

Density	kg/m3	constant	1135
Cp (Specific Heat)	j/kg-k	constant	2100
Thermal Conductivity	w/m-k	constant	0.23999999
Viscosity	kg/m-s	constant	0.0546
Molecular Weight	kg/kgmol	constant	62.0482

Thermal Expansion Coefficient	1/k	constant	0
Speed of Sound	m/s	none	#f

Material: air (fluid)

Property	Units	Method	Value(s)
Density	kg/m3	constant	1.225
Cp (Specific Heat)	j/kg-k	constant	1006.43
Thermal Conductivity	w/m-k	constant	0.0242
Viscosity	kg/m-s	constant	1.7894e-05
Molecular Weight	kg/kgmol	constant	28.966
Thermal Expansion Coefficient	1/k	constant	0
Speed of Sound	m/s	none	#f

Material: aluminum (solid)

Property	Units	Method	Value(s)
Density	kg/m3	constant	1350
Cp (Specific Heat)	j/kg-k	constant	0.80000001
Thermal Conductivity	w/m-k	constant	0.07

Cell Zone Conditions

Zones

name	id	type
fluid_coil_loop	4	fluid
soil_coil_loop	5	solid

Setup Conditions

fluid_coil_loop

Condition	Value
Material Name	ethylene-glycol
Specify source terms?	no
Source Terms	((mass)
(x-momentum) (y-momentum) (z-momentum) (energy))	
Specify fixed values?	no
Local Coordinate System for Fixed Velocities	no
Fixed Values	((x-
velocity (inactive . #f) (constant . 0) (profile)) (y-velocity (inactive . #f) (constant . 0) (profile)) (z-velocity (inactive . #f) (constant . 0) (profile)) (temperature (inactive . #f) (constant . 0) (profile)))	
Motion Type	0

X-Velocity Of Zone (m/s)	0
Y-Velocity Of Zone (m/s)	0
Z-Velocity Of Zone (m/s)	0
Rotation speed (rad/s)	0
X-Origin of Rotation-Axis (m)	0
Y-Origin of Rotation-Axis (m)	0
Z-Origin of Rotation-Axis (m)	0
X-Component of Rotation-Axis	0
Y-Component of Rotation-Axis	0
Z-Component of Rotation-Axis	1
Deactivated Thread	no
Porous zone?	no
Conical porous zone?	no
X-Component of Direction-1 Vector	1
Y-Component of Direction-1 Vector	0
Z-Component of Direction-1 Vector	0
X-Component of Direction-2 Vector	0
Y-Component of Direction-2 Vector	1
Z-Component of Direction-2 Vector	0
X-Component of Cone Axis Vector	1
Y-Component of Cone Axis Vector	0
Z-Component of Cone Axis Vector	0
X-Coordinate of Point on Cone Axis (m)	1
Y-Coordinate of Point on Cone Axis (m)	0
Z-Coordinate of Point on Cone Axis (m)	0
Half Angle of Cone Relative to its Axis (deg)	0
Relative Velocity Resistance Formulation?	yes
Direction-1 Viscous Resistance (1/m ²)	0
Direction-2 Viscous Resistance (1/m ²)	0
Direction-3 Viscous Resistance (1/m ²)	0
Choose alternative formulation for inertial resistance?	no
Direction-1 Inertial Resistance (1/m)	0
Direction-2 Inertial Resistance (1/m)	0
Direction-3 Inertial Resistance (1/m)	0
C0 Coefficient for Power-Law	0
C1 Coefficient for Power-Law	0
Porosity	1
Solid Material Name	hdpe

soil_coil_loop

Condition	Value

Material Name	loamy-soil
Specify source terms?	no
Source Terms	((energy))
Specify fixed values?	no
Fixed Values	((temperature (inactive . #f)
(constant . 0) (profile)))	
Motion Type	0
X-Velocity Of Zone (m/s)	0
Y-Velocity Of Zone (m/s)	0
Z-Velocity Of Zone (m/s)	0

Rotation speed (rad/s)	0
X-Origin of Rotation-Axis (m)	0
Y-Origin of Rotation-Axis (m)	0
Z-Origin of Rotation-Axis (m)	0
X-Component of Rotation-Axis	0
Y-Component of Rotation-Axis	0
Z-Component of Rotation-Axis	1
Deactivated Thread	no

Boundary Conditions

Zones

name	id	type
wall-7-shadow	19	wall
wall-7	7	wall
wall-18	18	wall
wall-17	17	wall
outer_fluid	14	interface
inner_soil	10032	interface
left_face	11	symmetry
right_face	10	symmetry
wall-soil_coil_loop	1	wall
top_face	8	wall
back_face	9	wall
bottom_face	12	wall
front_face	13	wall
inlet_fluid	15	velocity-inlet
outlet_fluid	16	pressure-outlet

Setup Conditions

wall-7-shadow

Condition	Value
Wall Thickness (m)	0
Heat Generation Rate (w/m3)	0
Material Name	hdpe
Thermal BC Type	3
Temperature (k)	300
Heat Flux (w/m2)	0
Convective Heat Transfer Coefficient (w/m2-k)	0
Free Stream Temperature (k)	300
Enable shell conduction?	no
Wall Motion	0
Shear Boundary Condition	0
Define wall motion relative to adjacent cell zone?	yes
Apply a rotational velocity to this wall?	no
Velocity Magnitude (m/s)	0
X-Component of Wall Translation	1
Y-Component of Wall Translation	0

Z-Component of Wall Translation	0
Define wall velocity components?	no
X-Component of Wall Translation (m/s)	0
Y-Component of Wall Translation (m/s)	0
Z-Component of Wall Translation (m/s)	0
External Emissivity	1
External Radiation Temperature (k)	300
Rotation Speed (rad/s)	0
X-Position of Rotation-Axis Origin (m)	0
Y-Position of Rotation-Axis Origin (m)	0
Z-Position of Rotation-Axis Origin (m)	0
X-Component of Rotation-Axis Direction	0
Y-Component of Rotation-Axis Direction	0
Z-Component of Rotation-Axis Direction	1
X-component of shear stress (pascal)	0
Y-component of shear stress (pascal)	0
Z-component of shear stress (pascal)	0
Surface tension gradient (n/m-k)	0
Specularity Coefficient	0

wall-7

Condition	Value

Wall Thickness (m)	0
Heat Generation Rate (w/m3)	0
Material Name	hdpe
Thermal BC Type	3
Temperature (k)	300
Heat Flux (w/m2)	0
Convective Heat Transfer Coefficient (w/m2-k)	0
Free Stream Temperature (k)	300
Enable shell conduction?	no
Wall Motion	0
Shear Boundary Condition	0
Define wall motion relative to adjacent cell zone?	yes
Apply a rotational velocity to this wall?	no
Velocity Magnitude (m/s)	0
X-Component of Wall Translation	1
Y-Component of Wall Translation	0
Z-Component of Wall Translation	0
Define wall velocity components?	no
X-Component of Wall Translation (m/s)	0
Y-Component of Wall Translation (m/s)	0
Z-Component of Wall Translation (m/s)	0
External Emissivity	1
External Radiation Temperature (k)	300
Rotation Speed (rad/s)	0
X-Position of Rotation-Axis Origin (m)	0
Y-Position of Rotation-Axis Origin (m)	0
Z-Position of Rotation-Axis Origin (m)	0
X-Component of Rotation-Axis Direction	0
Y-Component of Rotation-Axis Direction	0
Z-Component of Rotation-Axis Direction	1

X-component of shear stress (pascal)	0
Y-component of shear stress (pascal)	0
Z-component of shear stress (pascal)	0
Surface tension gradient (n/m-k)	0
Specularity Coefficient	0

wall-18

Condition	Value
-----	-----
Wall Thickness (m)	0
Heat Generation Rate (w/m3)	0
Material Name	hdpe
Thermal BC Type	1
Temperature (k)	300
Heat Flux (w/m2)	0
Convective Heat Transfer Coefficient (w/m2-k)	0
Free Stream Temperature (k)	300
Enable shell conduction?	no
Wall Motion	0
Shear Boundary Condition	0
Define wall motion relative to adjacent cell zone?	yes
Apply a rotational velocity to this wall?	no
Velocity Magnitude (m/s)	0
X-Component of Wall Translation	1
Y-Component of Wall Translation	0
Z-Component of Wall Translation	0
Define wall velocity components?	no
X-Component of Wall Translation (m/s)	0
Y-Component of Wall Translation (m/s)	0
Z-Component of Wall Translation (m/s)	0
External Emissivity	1
External Radiation Temperature (k)	300
Rotation Speed (rad/s)	0
X-Position of Rotation-Axis Origin (m)	0
Y-Position of Rotation-Axis Origin (m)	0
Z-Position of Rotation-Axis Origin (m)	0
X-Component of Rotation-Axis Direction	0
Y-Component of Rotation-Axis Direction	0
Z-Component of Rotation-Axis Direction	1
X-component of shear stress (pascal)	0
Y-component of shear stress (pascal)	0
Z-component of shear stress (pascal)	0
Surface tension gradient (n/m-k)	0
Specularity Coefficient	0

wall-17

Condition	Value
-----	-----
Wall Thickness (m)	0
Heat Generation Rate (w/m3)	0
Material Name	hdpe
Thermal BC Type	1

Temperature (k)	300
Heat Flux (w/m2)	0
Convective Heat Transfer Coefficient (w/m2-k)	0
Free Stream Temperature (k)	300
Enable shell conduction?	no
Wall Motion	0
Shear Boundary Condition	0
Define wall motion relative to adjacent cell zone?	yes
Apply a rotational velocity to this wall?	no
Velocity Magnitude (m/s)	0
X-Component of Wall Translation	1
Y-Component of Wall Translation	0
Z-Component of Wall Translation	0
Define wall velocity components?	no
X-Component of Wall Translation (m/s)	0
Y-Component of Wall Translation (m/s)	0
Z-Component of Wall Translation (m/s)	0
External Emissivity	1
External Radiation Temperature (k)	300
Rotation Speed (rad/s)	0
X-Position of Rotation-Axis Origin (m)	0
Y-Position of Rotation-Axis Origin (m)	0
Z-Position of Rotation-Axis Origin (m)	0
X-Component of Rotation-Axis Direction	0
Y-Component of Rotation-Axis Direction	0
Z-Component of Rotation-Axis Direction	1
X-component of shear stress (pascal)	0
Y-component of shear stress (pascal)	0
Z-component of shear stress (pascal)	0
Surface tension gradient (n/m-k)	0
Specularity Coefficient	0

outer_fluid

Condition	Value

inner_soil

Condition	Value

left_face

Condition	Value

right_face

Condition	Value

wall-soil_coil_loop

Condition	Value
-----	-----
Wall Thickness (m)	0
Heat Generation Rate (w/m3)	0
Material Name	aluminum
Thermal BC Type	1
Temperature (k)	300
Heat Flux (w/m2)	0
Convective Heat Transfer Coefficient (w/m2-k)	0
Free Stream Temperature (k)	300
Enable shell conduction?	no
Wall Motion	0
Shear Boundary Condition	0
Define wall motion relative to adjacent cell zone?	yes
Apply a rotational velocity to this wall?	no
Velocity Magnitude (m/s)	0
X-Component of Wall Translation	1
Y-Component of Wall Translation	0
Z-Component of Wall Translation	0
Define wall velocity components?	no
X-Component of Wall Translation (m/s)	0
Y-Component of Wall Translation (m/s)	0
Z-Component of Wall Translation (m/s)	0
External Emissivity	1
External Radiation Temperature (k)	300
Rotation Speed (rad/s)	0
X-Position of Rotation-Axis Origin (m)	0
Y-Position of Rotation-Axis Origin (m)	0
Z-Position of Rotation-Axis Origin (m)	0
X-Component of Rotation-Axis Direction	0
Y-Component of Rotation-Axis Direction	0
Z-Component of Rotation-Axis Direction	1
X-component of shear stress (pascal)	0
Y-component of shear stress (pascal)	0
Z-component of shear stress (pascal)	0
Surface tension gradient (n/m-k)	0
Specularity Coefficient	0

top_face

Condition	Value
-----	-----
Wall Thickness (m)	0
Heat Generation Rate (w/m3)	0
Material Name	loamy-soil
Thermal BC Type	0
Temperature (k)	278
Heat Flux (w/m2)	0
Convective Heat Transfer Coefficient (w/m2-k)	0
Free Stream Temperature (k)	300
Enable shell conduction?	no
Wall Motion	0
Shear Boundary Condition	0
Define wall motion relative to adjacent cell zone?	yes

Apply a rotational velocity to this wall?	no
Velocity Magnitude (m/s)	0
X-Component of Wall Translation	1
Y-Component of Wall Translation	0
Z-Component of Wall Translation	0
Define wall velocity components?	no
X-Component of Wall Translation (m/s)	0
Y-Component of Wall Translation (m/s)	0
Z-Component of Wall Translation (m/s)	0
External Emissivity	1
External Radiation Temperature (k)	300
Rotation Speed (rad/s)	0
X-Position of Rotation-Axis Origin (m)	0
Y-Position of Rotation-Axis Origin (m)	0
Z-Position of Rotation-Axis Origin (m)	0
X-Component of Rotation-Axis Direction	0
Y-Component of Rotation-Axis Direction	0
Z-Component of Rotation-Axis Direction	1
X-component of shear stress (pascal)	0
Y-component of shear stress (pascal)	0
Z-component of shear stress (pascal)	0
Surface tension gradient (n/m-k)	0
Specularity Coefficient	0

back_face

Condition	Value
-----	-----
Wall Thickness (m)	0
Heat Generation Rate (w/m3)	0
Material Name	loamy-soil
Thermal BC Type	1
Temperature (k)	300
Heat Flux (w/m2)	0
Convective Heat Transfer Coefficient (w/m2-k)	0
Free Stream Temperature (k)	300
Enable shell conduction?	no
Wall Motion	0
Shear Boundary Condition	0
Define wall motion relative to adjacent cell zone?	yes
Apply a rotational velocity to this wall?	no
Velocity Magnitude (m/s)	0
X-Component of Wall Translation	1
Y-Component of Wall Translation	0
Z-Component of Wall Translation	0
Define wall velocity components?	no
X-Component of Wall Translation (m/s)	0
Y-Component of Wall Translation (m/s)	0
Z-Component of Wall Translation (m/s)	0
External Emissivity	1
External Radiation Temperature (k)	300
Rotation Speed (rad/s)	0
X-Position of Rotation-Axis Origin (m)	0
Y-Position of Rotation-Axis Origin (m)	0

Z-Position of Rotation-Axis Origin (m)	0
X-Component of Rotation-Axis Direction	0
Y-Component of Rotation-Axis Direction	0
Z-Component of Rotation-Axis Direction	1
X-component of shear stress (pascal)	0
Y-component of shear stress (pascal)	0
Z-component of shear stress (pascal)	0
Surface tension gradient (n/m-k)	0
Specularity Coefficient	0

bottom_face

Condition	Value

Wall Thickness (m)	0
Heat Generation Rate (w/m3)	0
Material Name	loamy-soil
Thermal BC Type	0
Temperature (k)	288
Heat Flux (w/m2)	0
Convective Heat Transfer Coefficient (w/m2-k)	0
Free Stream Temperature (k)	300
Enable shell conduction?	no
Wall Motion	0
Shear Boundary Condition	0
Define wall motion relative to adjacent cell zone?	yes
Apply a rotational velocity to this wall?	no
Velocity Magnitude (m/s)	0
X-Component of Wall Translation	1
Y-Component of Wall Translation	0
Z-Component of Wall Translation	0
Define wall velocity components?	no
X-Component of Wall Translation (m/s)	0
Y-Component of Wall Translation (m/s)	0
Z-Component of Wall Translation (m/s)	0
External Emissivity	1
External Radiation Temperature (k)	300
Rotation Speed (rad/s)	0
X-Position of Rotation-Axis Origin (m)	0
Y-Position of Rotation-Axis Origin (m)	0
Z-Position of Rotation-Axis Origin (m)	0
X-Component of Rotation-Axis Direction	0
Y-Component of Rotation-Axis Direction	0
Z-Component of Rotation-Axis Direction	1
X-component of shear stress (pascal)	0
Y-component of shear stress (pascal)	0
Z-component of shear stress (pascal)	0
Surface tension gradient (n/m-k)	0
Specularity Coefficient	0

front_face

Condition	Value

Wall Thickness (m)	0
Heat Generation Rate (w/m3)	0
Material Name	loamy-soil
Thermal BC Type	1
Temperature (k)	300
Heat Flux (w/m2)	0
Convective Heat Transfer Coefficient (w/m2-k)	0
Free Stream Temperature (k)	300
Enable shell conduction?	no
Wall Motion	0
Shear Boundary Condition	0
Define wall motion relative to adjacent cell zone?	yes
Apply a rotational velocity to this wall?	no
Velocity Magnitude (m/s)	0
X-Component of Wall Translation	1
Y-Component of Wall Translation	0
Z-Component of Wall Translation	0
Define wall velocity components?	no
X-Component of Wall Translation (m/s)	0
Y-Component of Wall Translation (m/s)	0
Z-Component of Wall Translation (m/s)	0
External Emissivity	1
External Radiation Temperature (k)	300
Rotation Speed (rad/s)	0
X-Position of Rotation-Axis Origin (m)	0
Y-Position of Rotation-Axis Origin (m)	0
Z-Position of Rotation-Axis Origin (m)	0
X-Component of Rotation-Axis Direction	0
Y-Component of Rotation-Axis Direction	0
Z-Component of Rotation-Axis Direction	1
X-component of shear stress (pascal)	0
Y-component of shear stress (pascal)	0
Z-component of shear stress (pascal)	0
Surface tension gradient (n/m-k)	0
Specularity Coefficient	0

inlet_fluid

Condition	Value
-----	-----
Velocity Specification Method	2
Reference Frame	0
Velocity Magnitude (m/s)	1
Coordinate System	0
X-Velocity (m/s)	0
Y-Velocity (m/s)	0
Z-Velocity (m/s)	0
X-Component of Flow Direction	1
Y-Component of Flow Direction	0
Z-Component of Flow Direction	0
X-Component of Axis Direction	1
Y-Component of Axis Direction	0
Z-Component of Axis Direction	0
X-Coordinate of Axis Origin (m)	0

Y-Coordinate of Axis Origin (m)	0
Z-Coordinate of Axis Origin (m)	0
Angular velocity (rad/s)	0
Temperature (k)	268
is zone used in mixing-plane model?	no

outlet_fluid

Condition	Value
Gauge Pressure (pascal)	0
Backflow Total Temperature (k)	300
Backflow Direction Specification Method	1
Coordinate System	0
X-Component of Flow Direction	1
Y-Component of Flow Direction	0
Z-Component of Flow Direction	0
X-Component of Axis Direction	1
Y-Component of Axis Direction	0
Z-Component of Axis Direction	0
X-Coordinate of Axis Origin (m)	0
Y-Coordinate of Axis Origin (m)	0
Z-Coordinate of Axis Origin (m)	0
is zone used in mixing-plane model?	no
Radial Equilibrium Pressure Distribution	no
Specify targeted mass flow rate	no
Targeted mass flow (kg/s)	1
Upper Limit of Absolute Pressure Value (pascal)	5000000
Lower Limit of Absolute Pressure Value (pascal)	1

Solver Settings

Equations

Equation	Solved
Flow	yes
Energy	yes

Numerics

Numeric	Enabled
Absolute Velocity Formulation	yes

Relaxation

Variable	Relaxation Factor
Pressure	0.3
Density	1
Body Forces	1
Momentum	0.7

Energy 1

Linear Solver

Variable	Solver Type	Termination Criterion	Residual Reduction Tolerance
Pressure	V-Cycle	0.1	
X-Momentum	Flexible	0.1	0.7
Y-Momentum	Flexible	0.1	0.7
Z-Momentum	Flexible	0.1	0.7
Energy	Flexible	0.1	0.7

Pressure-Velocity Coupling

Parameter	Value
Type	SIMPLE

Discretization Scheme

Variable	Scheme
Pressure	Standard
Momentum	First Order Upwind
Energy	First Order Upwind

Solution Limits

Quantity	Limit
Minimum Absolute Pressure	1
Maximum Absolute Pressure	5e+10
Minimum Temperature	1
Maximum Temperature	5000